공학석사 학위논문

Flexural and Shear Performance of Angle Truss Composite Beams

앵글형 합성보의 휨 및 전단성능 평가

2018년 2월

서울대학교 대학원

건축학과

조 광 원

Flexural and Shear Performance of Angle Truss Composite Beams

지도 교수 박 홍 근

이 논문을 공학석사 학위논문으로 제출함

2018년 2월

서울대학교 대학원

건축학과

조 광 원

조광원의 공학석사 학위논문을 인준함

2018 년 2 월

위 원 장 _____ (인)

부위원장 _____ (인)

위 원 _____ (인)

Abstract

Flexural and Shear Performance of Angle Truss Composite Beams

Jo, Kwang won
Department of Architecture and Architectural Engineering
College of Engineering
Seoul National University

There is a lot of welcome for the precast construction method to reduce the labor in the field and to make it in the factory by upgrading the technology at the construction site and increasing the labor cost. As a structural member, various attempts have been made to increase the efficiency by using steel instead of using only conventional reinforcing bars and concrete which are conventionally used. This is a kind of encased composite beams that are used to construct a truss by using bending angle bent steel plates and casting a U-shaped precast on the bottom. Lower precast concrete replaces formwork to reduce field labor. It is then transported to the site and placed on a column, which is then integrated with the cast concrete. This system is economical because the effective depth of the cross section is deepened due to the existence of the inner angle truss, so that the amount of precast concrete can be drastically

reduced. Also, it has the merit that it can add convenience with light weight during construction.

The structural performance was verified through the bending and shear tests of the developed angle truss composite beams and compared with the predicted strength values of the existing design standards. In the bending test of the angle truss composite beams, it was found that it was well fitted when the design was made by the existing method which evaluated the bond strength, and the design bending strength was also obtained. However, excessive slippage occurred due to slip of the bolt in the proposed cross section. Further research is needed in this area. In the shear test, the web material of the angle truss embedded was calculated by shear reinforcement of ordinary reinforced concrete, and the experimental results were slightly less than or better than expected strength. The fracture modes of the specimens which were lower than the expected strength were different from diagonal tensile fracture. It was analyzed by the shear failure at the interface between upper and lower concrete of angle truss. In the case where adhesion failure does not occur, it is confirmed that the inner abdominal members are all surrendered, so that consideration can be given to the calculation of the shear strength. However, since the abdomen of the truss is connected by bolts, the upper limit of the shear strength is the bolt shear strength.

Through the evaluation of the structural performance, the flexural performance and the structural performance of a kind of embedded composite beam were confirmed, and it was concluded that the contribution of the internal steel to the shear strength of the embedded composite beam can be added.

Keywords : Encased composite member, Shear, Flexure, Prestressed beam, Precast concrete, Angle truss

Student Number : 2016-21088

Contents

List of Tables

List of Figures

List of Symbols

A_{a1} Area of single angle, mm^2

A_{sv} Area of steel vertical members, mm^2

A_{sd} Area of steel diagonal members, mm^2

A_{sa} Area of top or bottom steel chord members, mm^2

A_{sr} Area of bottom longitudinal reinforcements, mm^2

A_{tsr} Area of top longitudinal reinforcements, mm^2

A_v Area of transverse reinforcements, mm^2

A_1 Direct bearing area, mm^2

A_2 Area of effective bearing area, whose maximum is double times of A_1, mm^2

a/d Span and depth ratio

b_a Width of angle leg, mm

b_w Width of beam, mm

b_{bh} Length of below bolt hole, mm

b_{uh} Length of upper bolt hole, mm

d Effective depth of beam, mm

d_{cr} Depth of the center of top rebars, mm

d_{ta} Depth of the centroid of bottom angles, mm

d_{tr} Depth of the center of bottom rebars, mm

d_1 Total depth of upper concrete, mm

d_2 Distance from lower part concrete's top surface to the centroid of longitudinal reinforcements, mm

f_{ck} Concrete compressive strength (monolithic), MPa

$f_{ck,1}$ Upper part concrete's compressive strength, MPa

$f_{ck,2}$ Lower part concrete's compressive strength, MPa

f_{ya} Yield strength of top or bottom steel chord members, MPa

f_{yt} Yield strength of transverse reinforcements, MPa

f_{yr} Yield strength of longitudinal reinforcements, MPa

f_{ys} Yield strength of steel web members, MPa

M_{cre} Moment causing flexural cracking at section due to externally applied loads, $N \cdot mm$

r The center radiation of curved part

s The spacing of transverse reinforcements, mm

s_a The spacing of steel web members, mm

u One-forth center parameter of curved shape in singe angle $(=\frac{\pi r}{2})$, mm

V_c Concrete shear strength, N

V_s^* Shear strength of the steel section, N

V_{ci} Nominal shear strength provided by concrete when diagonal cracking results from combined shear and moment, N

V_{cw} Shear strength provided by concrete when diagonal cracking results from high principan tensile stress in web, N

$V_{diagonal}$ Shear strength of steel diagonal members in Angle truss

composite beams, N

V_{steel} Steel web members shear strength in Angle truss composite beams ($=V_{vertical}+V_{diagonal}$), N

$V_{stirrup}$ Shear strength of stirrups in Angle truss composite beams or Reinforced concrete beam, N

$V_{vertical}$ Shear strength of steel vertical members in Angle truss composite beams, N

$\overline{y_c}$ Depth of the centroid of top angles, mm

$\overline{y_t}$ Depth of the centroid of top angles, mm

α Angle defining the orientation of reinforcement

λ 1.0 for normal weight concrete

Chapter 1. Introduction

1.1 Background

Recently, the construction trend has been shifting toward a reduction in field labor due to an increase in the labor cost of the construction site. As a result, PC and steel structures are welcome.

Since the PC structure is manufactured in the factory, quality is maintained constantly and it is possible to make high-strength concrete. However, the weight of the PC structure becomes too heavy if you go to a heavy load span, which makes it very difficult to work with cranes used in existing construction sites. Also, there is a bit of a danger even if you put a PC booster that is raised as a general barge. In order to solve this inefficiency, Angle Composite was proposed.

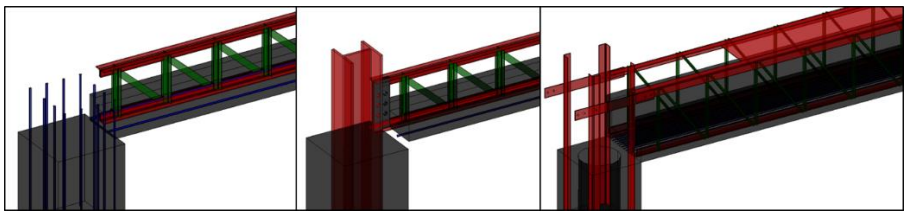

Figure 1-1 Angle truss composite beam connection with various column

Angle trusses to be assembled with bolts are arranged in the middle of the angle truss composite beams, and PCs are placed in the lower part to support the construction loads. It can be directly connected to the steel column at the

time of construction, and the weight is lightened to increase the convenience of construction.

Figure 1-1 shows the angle truss composite beam connection with various columns. Because angle truss composite beam has small amount of precast concrete, its weight is quietly lower than conventional precast girder.

Because the advantage of this is that the angle truss increases the section height, which increases the moment of inertia, which can drastically reduce the amount of concrete in the same PC. In addition, it is difficult to design the shear in the high load. I think that the inner angle truss contributes shear force.

1.2 Scope and Objectives

The objective of this study is to evaluate the structural performance of angle truss composite beam, which is one of composite systems that replaces the conventional PC and RC structures.

The bending test was carried out for the construction load and the permanent load. To perfectly bond between concrete and steel angle, the bearing strength can be calculated, which is introduced in ACI code provision. Its flexural capacity is determined by strain compatibility method in AISC code provision.

In shear tests, both normal reinforced concrete and prestressed concrete are used. Shear tests were performed to confirm the shear resistance of the inner angle truss. These strength assessments were based on AISC and ACI, and we would like to evaluate the reason why they can be expressed.

And the last chapter, the formulas for evaluating the flexural strength and shear strength of angle truss composite beams will be presented. The bending strength will be illustrated in the construction cross section and in the permanent section. Also, shear strength will be applied by emulating the method presented in the existing code. Therefore, the shear strength of concrete, stirrup, and steel will be added together.

1.3 Outline of the Master's Thesis

This thesis is divided into three main parts. Firstly, introduction of angle truss composite beam is presented. Angle truss composite beam which is the new system of composite member have several advantages to conventional system. To verify the flexural and shear performance of angle truss composite beams, each experiment was carried out. Based on the experimental results, the predicted strength equation is proposed. **Figure 1-2** briefly summarizes the entire contents of this thesis.

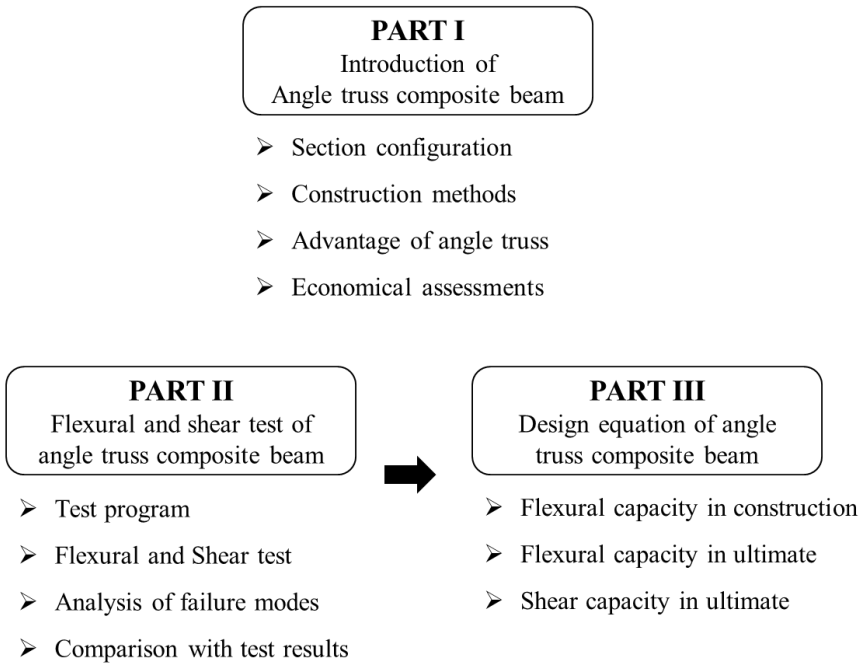

Figure 1-2 Outline of the master's thesis

PART I

In part I (chapter 3), the construction of a new system of angle truss composite beams will be described. In addition, angle truss composite beam has several advantages compared with existing RC systems and PC systems, and it will be compared with it. Economical assessment is performed to compare each construction methods. and it will show angle truss composite beam have the economical and construction advantages.

PART II

In order to evaluate the flexural and shear performance of the angle truss composite beams, sevral specimens were designed and tested. Each of the parameters will be introduced, the details of the specimens, and the experimental method will be explained. The experimental results will be compared with the predicted strength. Also strain gauge value will be summarized.

Part III

Based on the experimental results in part II, a design equation will be proposed for evaluating the flexural and shear performance of angle truss composite beams. The flexural performance is divided into a construction cross section and a permanent load section, and the shear performance will include the shear contribution of the inner angle truss. Also, we will introduce horizontal shear bond failure check.

Chapter 2. Literature Review

2.1 Code Review

2.1.1 Flexural strength provided by code provision

ANSI/AISC 360-10 [1] addresses composite members composed of rolled or built-up structural steel shapes and structural concrete acting together. The composite member is composed of encased composite members and filled compsite members. The topic of this paper, angle truss composite beam is a kind of encased composite members.

Flexural capacity

The encased composite member can be designed in both LRFD and ASD. In this paper, LRFD (the Load and Resistance Factor Design) will be used. The nominal flexural strength, M_n, shall be determined using one of the following methods:

(1) The superposition of elastic stresses on the composite section, considering the effects of shoring for the limit state of yielding (yield moment).

(2) The plastic stress distribution on the steel section alone, for the limit state of yielding (plastic moment) on the steel section.

(3) The plastic stress distribution on the composite section or the strain-compatibility method, for the limit state of yielding (plastic moment)

on the composite section. For concrete-encased members, steel anchors shall be provided.

In this research, angle truss portion of whole member section is a quite small. So strain compatibility method will be used to calculate flexural capacity of angle truss composite beam.

This method assumed that plane remains plane, means a linear distribution of strain with maximum concrete compressive strain equal to 0.003. Its advantage is posiblity of using non-linear material model.

Its basic assumption is the presence of shear anchor to integrate concrete and steel. In angle truss composite beam, vertical members of steel angle truss and bolts' head are acting as an shear anchor, which strength will be examined in next section.

2.1.2 Shear strength provided by code provision

ANSI/AISC 360-10 shows the shear strength of composite members. Angle truss composite beam, which is an encased composite member, can calculate the vertical shear strength in the following three ways.

(1) The available shear strength of the steel section alone

$$V_n = V_s^* \tag{2-1}$$

where, V_s^* is shear strength of the steel section.

(2) The available shear strength of the reinforced concrete portion (concrete plus steel reinforcement) alone as defined by ACI 318

$$V_n = V_c + V_{stirrup} \tag{2-2}$$

where, V_c is the shear strength of concrete.

$V_{stirrup}$ is the shear strength of the transverse reinforcements.

(3) The nominal shear strength of the steel section plus the nominal strength of the reinforcing steel

$$V_n = V_c + V_s^* \tag{2-3}$$

ACI 318M-11 [2] addresses the shear strength of reinforced concrete beams. Shear strength is composed of concrete portion and shear reinforcement portion.

$$V_n = V_c + V_{stirrup} \tag{2-2}$$

Normal Concrete shear strength

$$V_c = \frac{1}{6}\lambda\sqrt{f_{ck}}b_w d \tag{2-4}$$

Prestressed concret shear strength

$$V_c = \left(0.05\lambda\sqrt{f_{ck}} + 4.9\frac{V_u d}{M_u}\right)b_w d \geq \frac{1}{6}\lambda\sqrt{f_{ck}}b_w d \tag{2-5}$$

$$V_c = \min\left(V_{ci}, V_{cw}\right) \tag{2-6}$$

$$V_{ci} = 0.05\lambda\sqrt{f_{ck}}b_w d_p + V_d + \frac{V_i M_{cre}}{M_{\max}} \geq 0.17\lambda\sqrt{f_{ck}}b_w d \tag{2-7}$$

$$M_{cre} = \left(\frac{I}{y_t}\right)\left(0.5\lambda\sqrt{f_{ck}} + f_{pe} - f_d\right) \tag{2-8}$$

$$V_{cw} = \left(0.29\lambda\sqrt{f_{ck}} + 0.3 f_{pc}\right)b_w d + V_p \tag{2-9}$$

Shear reinforcement strength

$$V_{stirrup} = \frac{A_v f_{yt} d}{s} \tag{2-10}$$

When inclined reinforcements are used,

$$V_s = \frac{A_v f_{yt}\left(\sin\alpha + \cos\alpha\right)d}{s} \tag{2-11}$$

where, V_{ci} = nominal shear strength provided by concrete when diagonal cracking results from combined shear and moment, V_{cw} = nominal shear

strength provided by concrete when diagonal cracking results from high principan tensile stress in web, M_{cre} = moment causing flexural cracking at section due to externally applied loads, y_t = distance from centroidal axis of gross section, neglecting reinforcement, to tension face, α = angle defining the orientation of reinforcement.

2.1.3 Bearing strength

ACI 318M-11 shows that deseign bearing strength of concrete shall be dertermined by **Eq.(2-12)**.

$$B_n = 0.85 f_{ck} A_1 \left(\frac{A_2}{A_1} \right) \tag{2-12}$$

where, $A_1 = l_v l_h$, $A_2 / A_1 = 2$

The direct bearing area is A_1. When the supporting area is wider than A_1, the surrounding concrete confineds the bearing area, resulting in an increase in bearing strength. **Figure 2-1** illustrates the application of the frustum to find A_2.

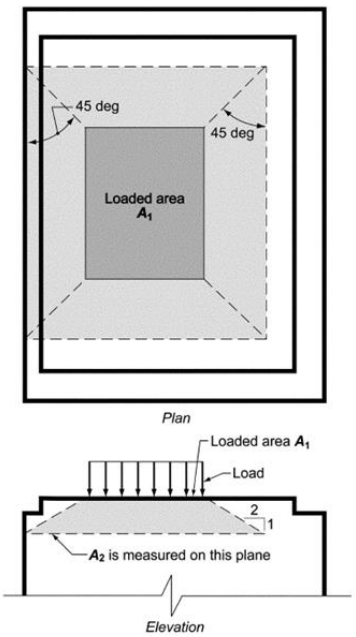

Figure 2-1 Determination of A_2 in stepped or sloped supports

2.2 Literature Review

2.2.1 Flexural test for encased composite beam

Eom et al. [3] proposed a prefabricated steel-reinforced concrete column called PSRC. The bending performance was tested. In order to predict the bending performance, the bending strength was calculated as the compatibility method of the strain. In addition, the predicted strength curve was also drawn using the nonlinear material model and the experimental results were very similar to the predicted values. The adhesion between angle and concrete was considered to be caused by tie reinforcement welded to the angle, and this formula was proposed.

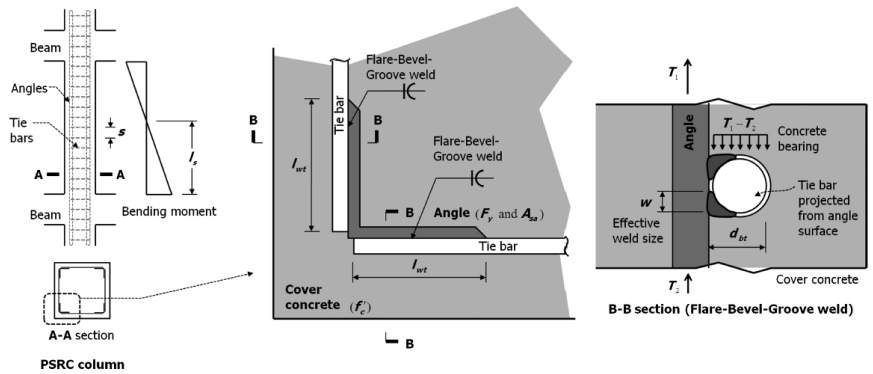

Figure 2-2 Bearing strength of PSRC columns

$$B_n = \alpha\left[0.85 f_c'\left(2 d_{bt} l_{wt}\right)\right]\left(\frac{l_s}{s}\right) \tag{2-13}$$

To calculate the bearing strength, bearing area was defined. The bearing area (A_1) is determined by tie bar area which is directly attached to steel angle (**Figure 2-2**). And also, area multiplier value is considered as 2.0 (the maximum value in code provision) which is proposed by **Eq.(2-13)**. And its bearing strength was well with test results.

2.2.2 Vertical shear strength of composite concrete beams

Kim et al. [4] tested the shear strength of composite beams with dual concrete without transverse reinforcements. The main test parameters used were the area ratio of HSC (High Strength Concrete) to LSC (Low Strength Concrete), the flexural reinforcement ratio, and the shear span-depth ratio. total 16 specimens were tested. And the results show that ACI 318 code's prediction equation is some underestimate the test results. And proposed the design equation to predict the vertical shear strength of dual concrete beams.

Kim et al. [5] also tested the shear strength of composite beams with dual concrete with transverse reinforcements. The main test parameters used were the area ratio of HSC (High Strength Concrete) to LSC (Low Strength Concrete), the flexural reinforcement ratio, and the shear span-depth ratio. total 15 specimens were tested. And the results show that ACI 318 code's prediction equation indicated the differences with test results. In calculation of ACI 318 strength, the sum of upper concrete's shear strength and lower concrete's shear strength is used. And modified method which contained failure degress is well matched with the test results.

2.2.3 Horizontal shear strength of composite concrete beams

Loov et al. [6] proposed horizontal shear strength of composite concrete beams with a rough interface. Previously, Mattock et al. [7] have been conducting extensive studies on horizontal shear strength. In addition to this, additional experiments were carried out and the horizontal shear strength equation was proposed as **Eq.(2-14)**. The proposed equation and the results of several previous researchers are presented in **Figure 2-3**.

$$v_n = k\sqrt{\left(0.1+\rho_v f_y\right) f_c'} \le 0.25 f'_c \tag{2-14}$$

The proposed formula conservatively evaluates the horizontal shear strength, which implies that horizontal shear failure may not occur even if the strength is insufficient. The horizontal shear strength is to be checked during the angled compositebeam shear test through **Eq.(2-14).**

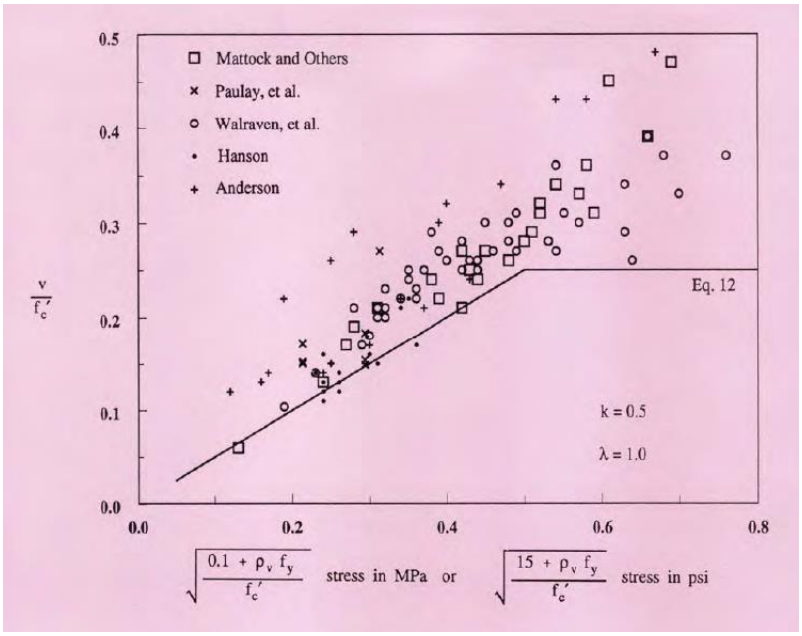

Figure 2-3 The comparison of the suggested equation with the results

Chapter 3. Construction Method for Angel Truss Composite Beams

3.1 Construction methods of angle truss composite beams

The construction method of angle truss composite beams is as follows :

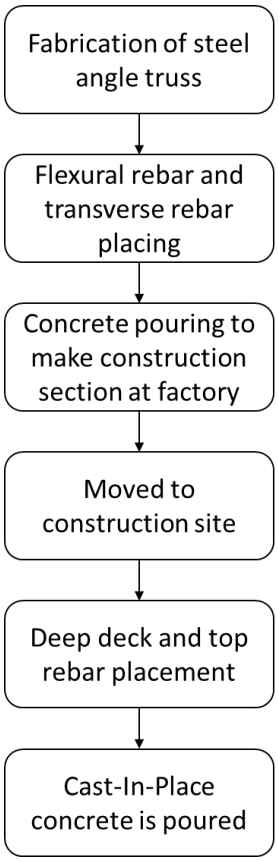

Figure 3-1 Construction procedure of angle truss composite beam

Figure 3-1 shows construction procedure of angle truss composite beams, steel angle truss is fabricated first. And then it moves to precast producer. The angle truss assembled at the factory is integrated into the precast concrete with the bottom reinforcements (rebars or strands). At this time, the lower precast concrete is able to obtain economical efficiency because it reduces the volume against the normal precast system.

Afterwards, the constructed cross section is moved to the site and mounted like a PC beam. Since the amount of the PC is greatly reduced, there is an advantage that the workability is facilitated. The deck is raised in the field, the upper reinforcing bars are arranged, and cast-in-place concrete is integrated and finished.

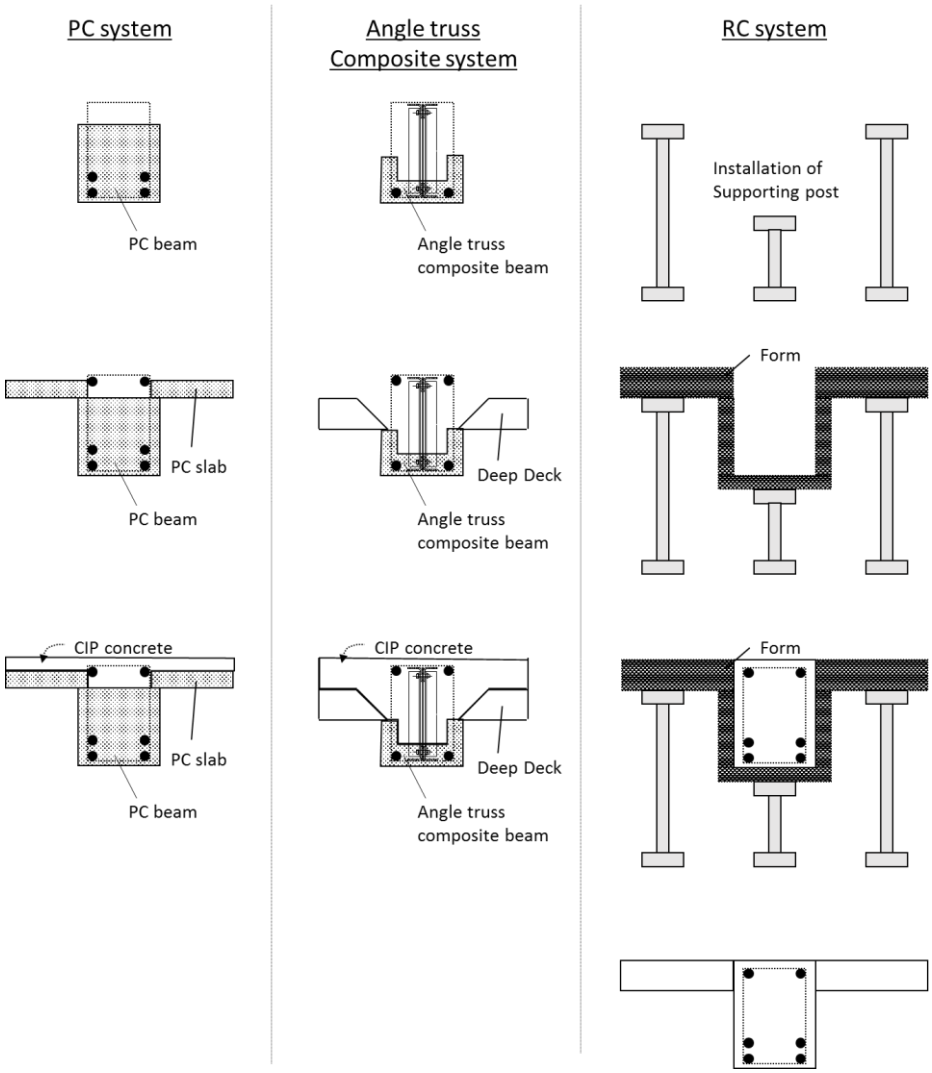

Figure 3-2 Comparison of angle truss composite beam with precast concrete and conventional reinforced concrete structure

From Figure 3-2, the construction procedures can be compared. Angle truss composite beam has a lot of advantage.

As such, the angle truss composite beam is similar to the PC construction method. However, since the amount of PC is remarkably small, convenience of construction is increased, and there is an advantage of economical part.

And if you compare it with RC, there is no formwork and the eastern part, you can reduce the labor cost by reducing the field work, and the construction phase is shortened, which helps to shorten the construction time.

3.2 Construction of Specimens

Procedures of making the test specimens are illustrated in **Figure 3-3**. Firstly, Steel angle and plate are produced. The cutting and bending work were carried out according to the designed size. Laser cutting machine is used for cutting work and press brake machine is used for bending to make cold-formed steel angle.

Second, Angle trusses were assembled before placing reinforcing bars according to the drawings. Bolt connection or welding connection was used in assembling trusses. After that, strain gauges are located on the angle truss member, longitudinal rebar and transverse rebar.

Figure 3-4 showed the locations of strain gauge in flexural specimens and shear specimens.

Third, Molding was fabricated and place the fabricated angle truss and rebars. Last, concrete was poured to be careful not to damage to the gauges. Also, concrete cylinders (diameter = 100mm and height = 200mm) were made to perform compression test.

<Pressing steel plate to angle>

<Fabrication of Steel Angle Truss>

<Manufacturing molds>

<Placing concrete>

Figure 3-3 Construction procedures of angle truss composite beam.

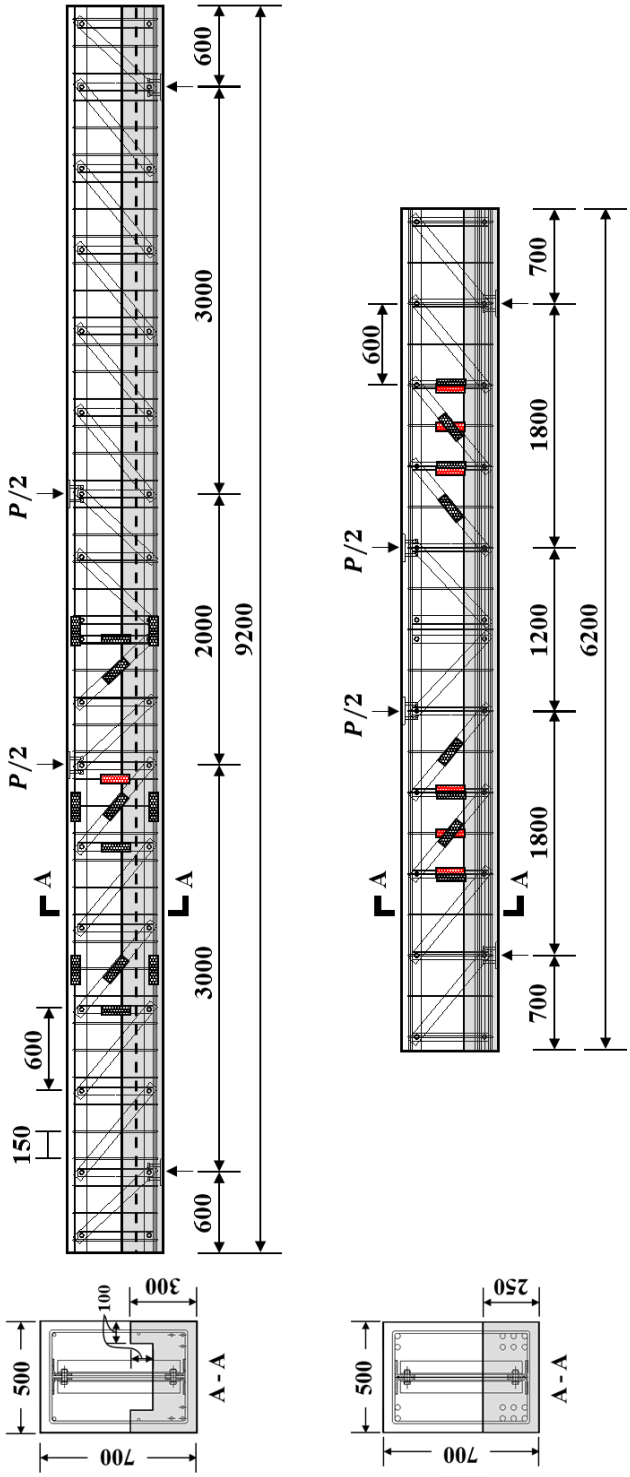

Figure 3-4 Strain gaugle location of 9.2m specimen(flexure) and 6.2m specimen (shear specimen)

3.3 Economical Assessment of Angle Truss Composite Beam

An economic analysis was conducted on typical units of 11m x 11m span in five cases which consist of conventional reinforced concrete system, steel+SRC system, precast system I, precast system II, angle truss composite system.

Table 3-1 illustrates the comparison of section, typical precast girder with angle truss composite beam. PC quantity which is shaded area, reduce quietly. Actually, 48% of pc quantity can be reduced using angle truss composite beam substituting for pc girder. Reduction of PC quantity result in economical advantages. Ths advantage may compensate for the economic losses that have already occurred in fabrication of angle truss.

Table 3-1 The comparison typical PC girder with Angle truss Composite beam

	ENDs	CEN
PC Girder	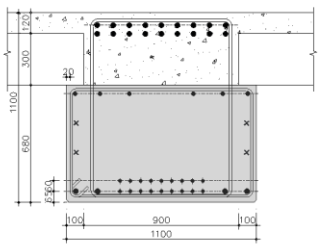	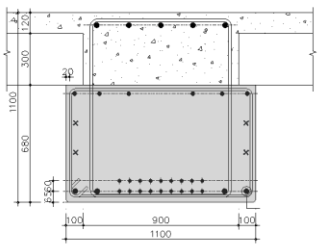
Angle Truss Composite Beam	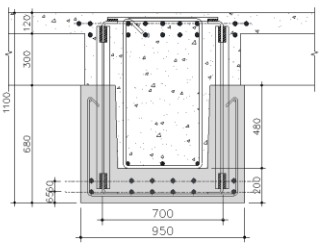	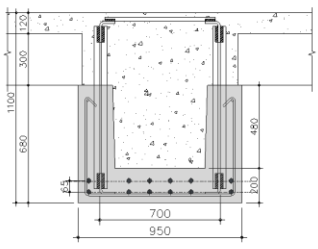

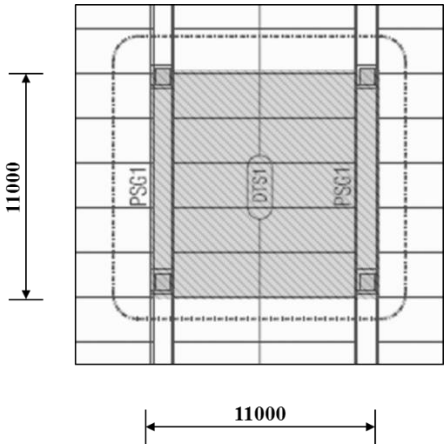

Figure 3-5 The review plan (11m span)

The review plan is illustrated in **Figure 3-5**. It is based on an 11m x 11m unit with $20 kN/m^2$ live load, which is the basic unit of the warehouse. The loading conditions were the same for all cases, and the angle truss composite beam system was calculated under the condition that angle truss composite beams, angle truss composite columns (developed), and the existing PC slabs were used. The amount of reduction in the girder has been considerable.

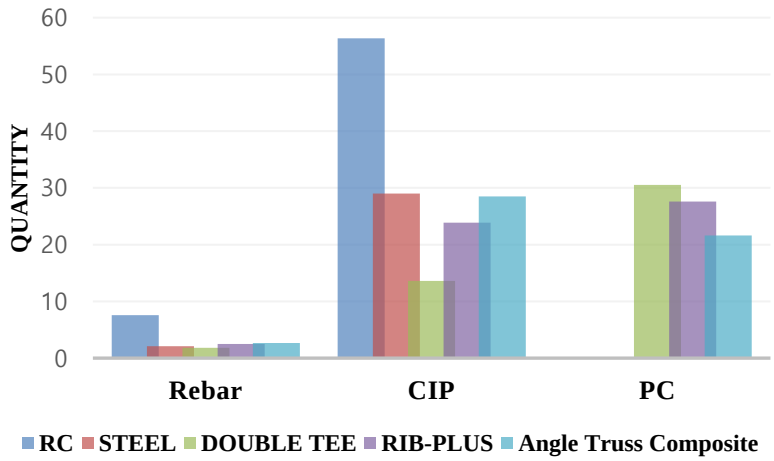

Figure 3-6 Comparison of quantity by construction method

Figure 3-6 shows the comparison of quantity by each case. Precast quantity of angle truss composite beam is lowest in all cases. And its reduction is added to cast-in-place concrete (CIP). And **Figure 3-7** indicates the total unit cost of construction in 11m x 11m span. Angle truss composite system has economical advantages than reinforced concrete and steel system. And is as cheap as precast system.

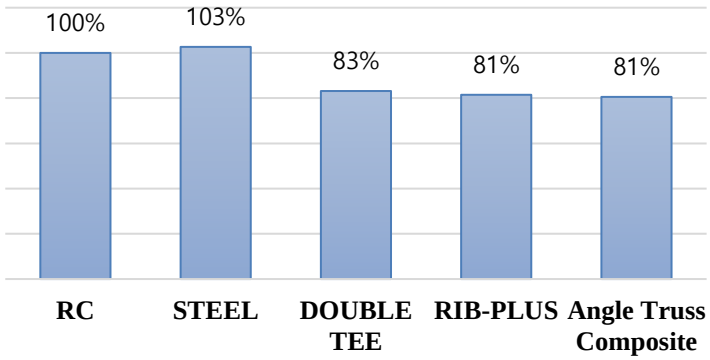

Figure 3-7 Cost comparison by construction methods

Chapter 4. Flexural Test for Angle Truss Composite Beams

4.1 Introduction

Angle truss composite beam is a kind of encased composite beam defined in AISC. Encased composite beam's flexural strength can be determined by strain compatibility method. In order to use strain compatibility method, the composite section should linear strain distribution. That is, adhesion of steel and concrete is essential.

In this chapter 4, The flexural specimens are constructed and tested. In designing specimens, bond strength will be calculated by bond strength equation in ACI 318.

4.2 Flexural Theory for Composite Section

Angle truss composite beam is a kind of concrete-encased steel composite section (CES). Steel angle truss is located at center of precast beam section with cover thickness. It is called construction section. (**Figure 4-1**(a)) The construction section is unified with cast-in-place concrete with steel deck in construction site. Therefore, steel angle truss is fully buried in concrete. (**Figure 4-1**(b))

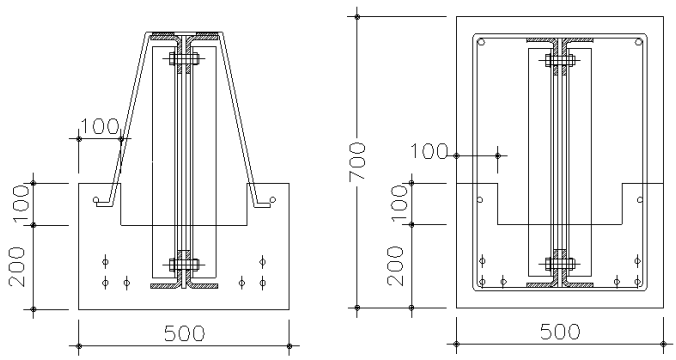

Figure 4-1 Angle truss composite beam section

AISC code provision suggests two methods for calculation of flexural capacity of Concrete-encased steel composite section. The first one is plastic stress distribution method; the other is strain compatibility method. In this section, strain compatibility method will be presented where perfectly bonded state is assumed.

To meet the perfect bond state, shear transfer between steel angle truss and concrete is also covered for the basic assumption of strain compatibility method

from ACI code provision.

4.2.1 Strain Compatibility Method for Composite Member

ANSI/AISC 360-10, Specification for Structural Steel Buildings

Sect. I1. 2. Nominal Strength of Composite Sections

The nominal strength of composite sections shall be determined in accordance with the plastic stress distribution method or the strain compatibility method as defined in this section.

2b. Strain compatibility method

For the strain compatibility method, a linear distribution of strains across the section shall be assumed, with the maximum concrete compressive strain equal to 0.003 mm/mm. the stress-strain relationships for steel and concrete shall be obtained from tests of from published results for similar materials.

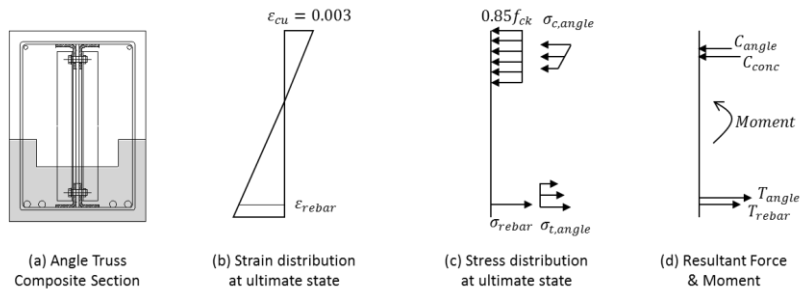

Figure 4-2 Strain compatibility on Angle Truss Composite Section

Figure 4-2 shows the strain compatibility method for steel angel truss composite section. Steel angle was assumed to be perfectly bond to concrete. The bond strength will be covered next section.

the neutral axis depth is determined through force equilibrium condition. Neutral axis depth, c can be determined from **Eq.(4-1)**

$$0.85 f_{ck} ab + \sigma_{cr} A_{sr} + \sigma_{ca} A_{sa} = \sigma_{tr} A_{tsr} + \sigma_{ta} A_{sa} \quad (4\text{-}1)$$

where, f_{ck} = concrete strength, $a = \beta_1 c$, b = beam width, σ_{cr} = compressive stress in upper rebar, σ_{ca} = compressive stress in upper angle, σ_{tr} = tensile stress in bottom rebar $(\leq f_{yr})$, σ_{ta} = tensile stress in bottom angle $(\leq f_{ya})$, and A_a = area of double angle.

After determination of neutral axis depth, moment capacity can be calculated by **Eq.(4-2)**

$$\begin{aligned} M_n = {} & C_c\left(\frac{h}{2}-\frac{a}{2}\right) + C_r\left(\frac{h}{2}-d_{cr}\right) + C_a\left(\frac{h}{2}-d_{ca}\right) \\ & + T_a\left(\frac{h}{2}-d_{ta}\right) + T_r\left(\frac{h}{2}-d_{tr}\right) \end{aligned} \quad (4\text{-}2)$$

where, h = beam depth, and d_{cr} , d_{ca} , d_{tr} , d_{ta} are the distance of upper rebar center, upper double angle's centroid, bottom rebar center, bottom double angle's centroid from the extreme top fiber, respectively.

4.2.2 Bond strength between steel angle and concrete

Concrete bearing strength is defined in ACI code provision. Design bearing strength of concrete shall not exceed φ (0.85fc′A1), except when the supporting surface is wider on all sides than the loaded area, then the design bearing strength of the loaded area shall be permitted to be multiplied by but by not more than 2.

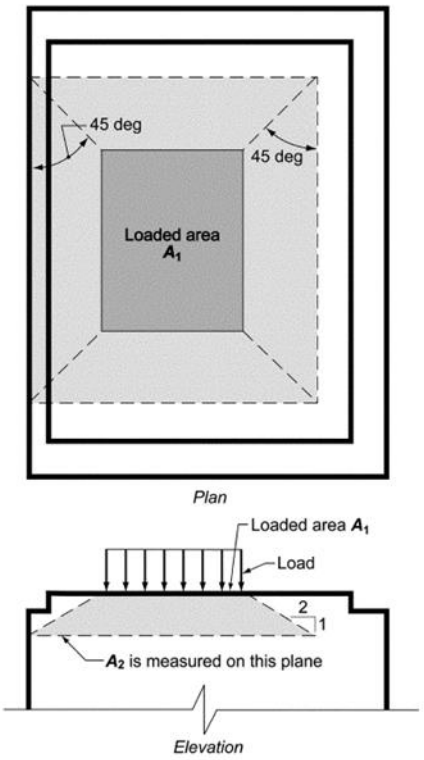

Fig. R10.14—Application of frustum to find A_2 in stepped or sloped supports.

Figure 4-3 The loaded area for calculation of bearing area

And Eom et al.[3] used this concept to calculated bond strength between steel angle and concrete applying A2/A1 is 2.

So, **Eq.(4-3)** can be derived from ACI code.

$$B_n = 0.85 f_{ck} A_1 \left(\frac{A_2}{A_1} \right) \tag{4-3}$$

where, $A_1 = l_v l_h$ and, $A_2 / A_1 = 2$

4.3 Variables

The purpose of this experiment is to evaluate the flexural performance of angle truss composite beam. In this test, both construction section and ultimate secntion will be tested. The main variables are objective target (e.g. construction load, permanent load) and the placement of prestressing on the lower precast part. Specimens' section and variables are listed in **Figure 4-4** and **Table 4-1.**

Table 4-1 Configures the experimental variables

Specimens	Objective Target	Dimension (mm x mm)	f_{ck} (MPa)	Prestressing stress (MPa)
PSC-F1	Construction load	U shape concrete	60 (bottom)	$0.75f_{pu}$
PSC-F2	Ultimate load	500 x 700	24 (top) / 60 (bottom)	
RC-F3				-

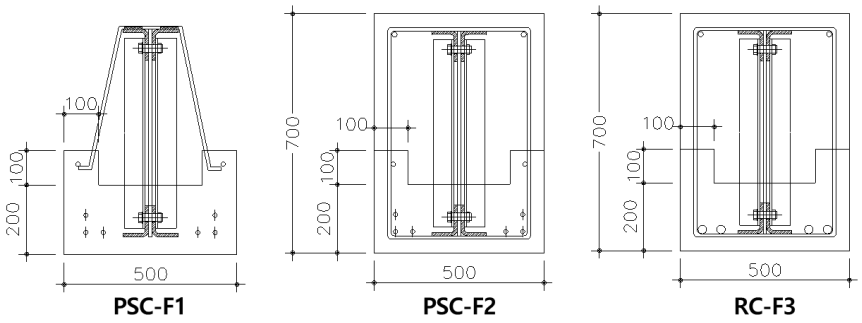

Figure 4-4 the section of flexural specimens

PSC-F1 is a construction section, which is designed to withstand construction loads. After assembling the steel angle truss, prestressed force is given to the lower part concrete. The side wing parts were welded to provide support for lateral buckling. In addition, stirrups were removed for ease of fabrication because they do not play a role in the experiment.

PSC-F2 is a ultimate load section of PSC-F1, and the lower part is designed at PSC and the upper part is cast-in-place concrete. The shear resistance is designed assuming that the concrete and stirrup are fully resisted. The shear performance of angled composite beams will be discussed further in the next section.

RC-F3 is a ultimate load section same as PSC-F3. The difference is that lower part concrete is not prestressed concrete but normal precast concrete.

4.4 Specimen Design

All specimens were designed so that flexural failure takes precedence. Flexural strength is determined by Section 4.1.1 and Bond strength is calculated by section 4.1.2. The lower part concrete strength was designed at 60MPa and the upper part concrete at 24MPa to reflect the trend of high strength of concrete. The whole dimension of the beam section was 500 mm x 700 mm. and PSC-F1 specimen had U shape concrete section. Because construction section was simulating the actual construction section.

In the specimens, D25 bars (bar diameter $d_b = 25.4mm$ and yield strength $f_y = 500MPa$) and D10 bars (bar diameter $d_b = 10.7mm$ and yield strength $f_y = 400MPa$) were used for the longitudinal and transverse reinforcements, respectively. Steel angle and plate were ATOS60 (SM 570) is used.

12.7mm SWPCBL strands (yield strength $f_y = 1680MPa$, ultimate strength $f_u = 1860MPa$) were used for prestress. And the prestessing force is 75% of ultimate strength of strands.

Angle Truss Design

The design of the angle truss was conducted in the following manner. First objective is that the angle truss can be develop to plastic moment. Because shear span is 3m, maximum load developing platic moment is calculated by **Eq.(4-4)**

$$P_{max} = \frac{2}{3} M_{plastic} = 411.7kN \tag{4-4}$$

All members and bolt connections were designed to resist the internal force before the plastic moment. Member's force can be calculated by truss action. Vertical member is under compressive force and diagonal member is under tensil force in pratt truss. Their force are **Eq.(4-5)** and **(4-6)** repectively. (compression is negative.)

$$P_{vertical} = -\frac{P_{max}}{2} = -205.9kN \tag{4-5}$$

$$P_{diagonal} = \frac{P_{max}}{2sin\theta} = 268.0kN \tag{4-6}$$

From AISC-360, Vertical member (2L-60x60-6T, 550mm) and diagonal member (PL-70-10T) are able to resist maximum load.

Each element is combined by bolt connection. To transfer internal forces between elements, F10T M22 bolt is used.

PSC-F1 (Construction, Prestressed Specimen)

PSC-F1 consists of bottom precast concrete with prestressing and steel angle truss. It has 2 states of failure modes. First one is construction state, which is to resist constrction load. And construction failure mode is defined as 60% yield of top chord. The other one is ultimate state, which is not real state. But for the purpose of analysis of force distribution. Ultimate failure mode is defined as 100% yield of top chord. In case of LTB (lateral torsional buckling), the ultimate load cannot be reached.

Effective prestressed force is 75% of ultimate strength of strand (**Eq.(4-7)**). And ε_1 can be calculated by **Eq.(4-8)**

$$f_{pe} = -0.75 f_{up} = 1395MPa \tag{4-7}$$

$$\varepsilon_1 = \frac{f_{pe}}{E_p} = -0.006975 \tag{4-8}$$

Because the centroid of strands is not equal to the centroid of concrete section, eccentricity is applied. (**Eq.(4-9),(4-10)**)

$$f_2 = \frac{P_e}{A_p} + \frac{M \cdot y}{I_p} = \frac{P_e}{A_c} + \frac{P_e \cdot e_p \cdot y}{I_c} \tag{4-9}$$

$$\varepsilon_2 = \frac{f_2}{E_p} \tag{4-10}$$

Finally, when load is at certain point, concrete extreme tensile fiber is changed to tensile strain. Iteration calculation is required to meet force equilibrium using **Eq. (4-11),(4-12),(4-13)**

$$\varepsilon_3 = \frac{0.003}{c}\left(c - d_p\right) \tag{4-11}$$

$$\varepsilon = \varepsilon_1 + \varepsilon_2 + \varepsilon_3 \tag{4-12}$$

$$f_{ps} = \begin{cases} E_p \cdot \varepsilon \ (\varepsilon \le \varepsilon_y) \\ 6767 \cdot \varepsilon - 1623 \ \ (\varepsilon_u \le \varepsilon \le \varepsilon_u) \end{cases} \tag{4-13}$$

Especially, PSC-F1 didn't have concrete in compression. So, top chord compressive force is only resist compression. The above processes were summarized in **Figure 4-5**.

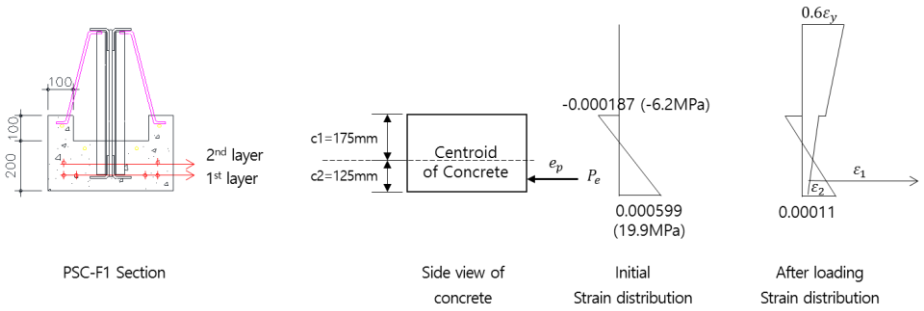

Figure 4-5 Flexural strength calculation procedure of PSC-F1

PSC-F2

PSC-F2 is composited by PSC-F1 and upper concrete. So, it is a kind of encased composite concrete beam. Its flexural strength can be calculated by same procedure of PSC-F1. But upper concrete also resist compressive force.

The results are that neutral axis depth (c) is 158mm. and moment capacity is 1328.6kN-m when concrete strain is 0.003 using equivalent stress block.

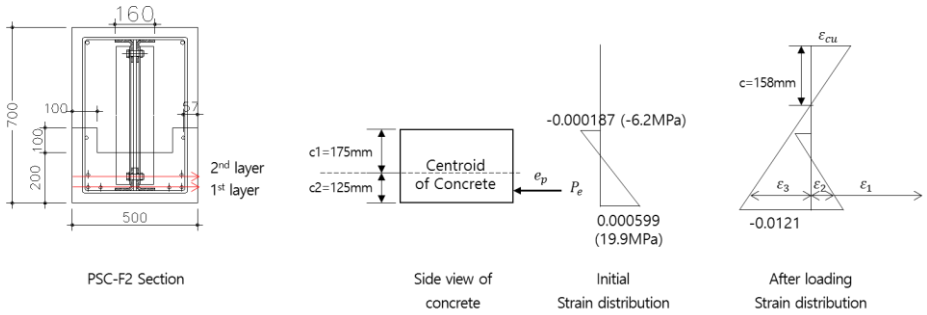

Figure 4-6 Flexural strength calculation procedure of PSC-F2

And shear strength of prestressed beam is usually greater than reinforced concrete beam. To cause bending failure first, shear strength is greater than flexural strength. So concrete shear strength is calculated by **Eq.(4-14), (4-15)** conservatively.

$$V_c = \frac{1}{6}\sqrt{f_{ck}}b_w d = 319kN \tag{4-14}$$

$$V_n = V_c + V_s = 591.6kN \tag{4-15}$$

RC-F3

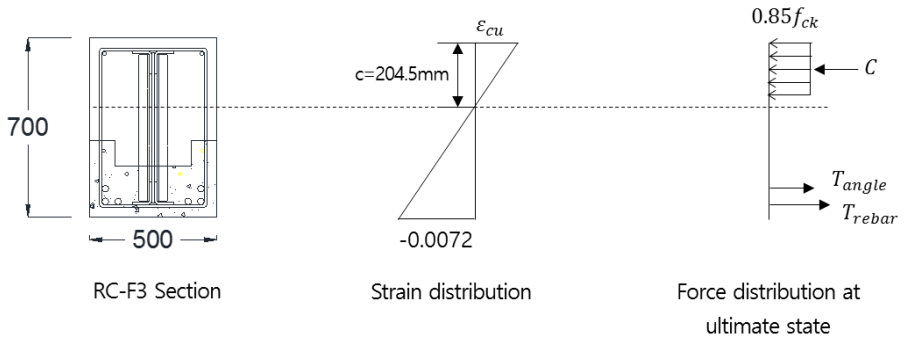

Figure 4-7 Flexural strength calculation procedure of RC-F3

Moment capacity can be calculated almost same with normal reinforced concrete beam. The different thing is that angle has area at centroid of that angle. And steel angle is assumed to be bond perfectly.

In that case, flexural strength can be demonstrated by **Eq.(4-16)**

$$M_n = C_{conc}\left(\frac{h}{2}-\frac{a}{2}\right) + C_r\left(\frac{h}{2}-d_{cr}\right) + C_a\left(\frac{h}{2}-d_{ca}\right) + T_a\left(\frac{h}{2}-d_{ta}\right) + T_r\left(\frac{h}{2}-d_{tr}\right) = 1330kN\cdot m \quad (4\text{-}16)$$

The shear strength of RC-F3 is noremal reinforced concrete. To cause bending failure first, shear strength is greater than flexural strength. So concrete shear strength is calculated by **Eq.(4-17)**

$$V_n = V_c + V_s = 591.6kN \quad (4\text{-}17)$$

Bearing Strength

Bearing strength on one beraing surface can be calculated by **Eq.(2-1)**

$$B_n = 0.85 f_{ck} A_1 \left(\frac{A_2}{A_1}\right) \tag{2-1}$$

In flexural specimen, Since the bearing surface is arranged at intervals of 600mm along the section of shear span 3000mm, there are 5 bearing surfaces in total. Finally, the nominal bearing strength shall be determined by **Eq.(4-18)**

$$B_n = 0.85 f_{ck} A_1 \left(\frac{A_2}{A_1}\right)\left(\frac{a}{s}\right) = 734.4kN \tag{4-18}$$

The required bearing strength generated by bearing of the vertical member is the yield of the angle. The value is by **Eq.(4-19)**

$$B_u = A_{sa} F_{ya} = 565kN \tag{4-19}$$

Therefore, it is possible to secure the bondage strength by **Eq.(4-20)** in all angle truss composite beam bending specimens. When the value of B_n/B_u is greater than 1, angle truss is confirmed to bond completely.

$$\frac{B_n}{B_u} = 1.30 \tag{4-20}$$

Summary

The overall design results are summarized in **Table 4-2.**

Table 4-2 Flexural specimens design results

Specimens		Prestressing stress (MPa)	M_n (kN · m)	V_n (kN)	B_n/B_u	Predicted failure mode
PSC-F1	Construction load	$0.75f_{pu}$	298.3	-	1.30	60% yield of top chord
	Maximum load		168.4	-		
PSC-F2			1328.6	591.6		Flexural failure (Concrete crushing)
RC-F3		-	1330.0			

4.5 Specimen Detail

Figure 4-8 shows details of test specimens for evaluating the flexural performance of angled composite beams.

Angle trusses were first assembled and then buried with concrete. To prevent slipping of the bolt during the test, the clearance of the bolt hole was reduced to 1 mm, and the surface of the steel was blasted to use slip-critical connection. The members of the angle truss are as follows. (**Table 4-3**)

Table 4-3 The properties of the angle truss members

Member	Top / Bottom Chord	Vertical member	Diagonal member
Material	ATOS 60	SS400	ATOS 60
Size	2L-90x75-10T	2L-60x60-6T	PL-80-10T

PSC-F1 placed concrete under the U-shape at the bottom and gave a prestress force. At this time, the lower part of the angle truss was embedded in the center of the specimen. In order to prevent lateral buckling, the lateral buckling prevention steel plate was attached to the lower PC and the upper angle was tack welded.

PSC-F2 is a section of ultimate load of PSC-F1, which is unified by cast-in-place concrete. To resist shear demand, D10 stirrups were placed at 150mm.

RC-F3 is a cross-section supporting permanent load same as PSC-F2, but a general PC is used without PSC at the bottom.

The material strengths used in the test specimens are as follows.

Table 4-4 Composition and properties of concrete mixtures

f_{ck} (MPa)	W/C (%)	s/(a+s) (%)	a_{max} (mm)	Weight of unit volumn (kg/m^3)				
				W	C	s	a	AD
24	47.8%	47.0%	25	170	356	848	956	3.2
60	24.2%	43.9%	25	160	660	727	929	7.26

Table 4-5 Tensile test results of rebars

Steel grade	Bar size	Area (mm^2)	Yield stress f_y (MPa)	tensile stress f_u (MPa)
SD400	D10	71	457	602
SD600	D25	507	537	693

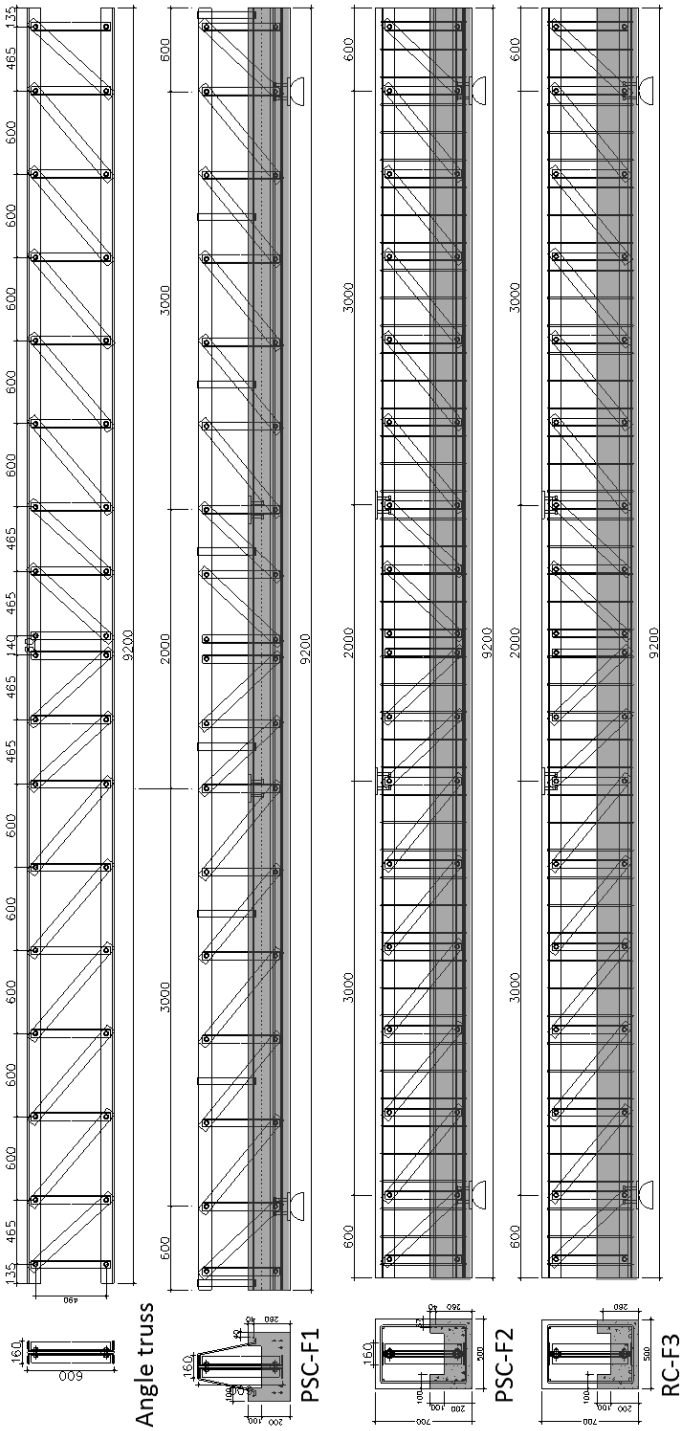

Figure 4-8 Flexural specimens detail

4.6 Test Method

The flexureal test was performed at 4 points. The total length of the test specimen was 9.2 m and the test force was applied using a 2 m span jig for 2 - point loading. The support was composed of rollers, each located 600 mm from the end of the specimen. (**Figure 4-9**) That is, the shear span is 3000mm and the effective depth of the test specimen is 650mm, and the shear span ratio is a / d = 4.5.

The experimental speed was 0.03 mm / sec, and strain gauges were installed on the angled truss and inner reinforcement. Data measurements were taken every second. In the middle of the experiment, the experiment was stopped to draw cracks on the concrete, and then reloaded.

In order to measure the displacement, 5 LVDTs (The linear variable differential transformer) were installed at 1000mm interval in the below part of the specimen. LVDTs were measured with bar.

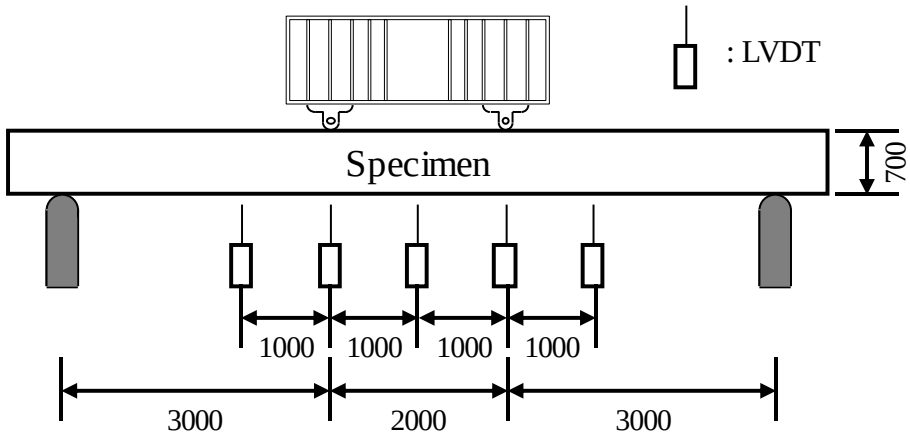

Figure 4-9 Flexural test setup of angle truss composite beam

4.7 Test Results

4.7.1 Load-Displacement Relationship

A total of three bending tests were carried out. The experimental results are summarized in **Table 4-6**. The PSC-F1 specimen is a construction section in which a PSC is introduced while a precast concrete is installed only at the bottom, and an angle truss is disposed at the center. The PSC-F2 specimen is a ultimate section of PSC-F1. It is united with cast-in-place concrete. The PSC-F3 specimen is also a ultimate section. But doesn't have prestressing force. It used normal precast concrete at lower part.

Overall, all specimens were similar or better test strength than expected strength. The PSC-F1 showed large deflection than expected due to excessive slip at bolt connection. PSC-F2 and Rc-F3 showed ductile behavior and reached expected bending strength. These results show that the steel angles are fully attached to the concrete by bearing strength.

Table 4-6 Angle Truss Composite beam flexural test results

Specimen		Predicted strength		Test strength		Strength ratio	Failure mode
		M_n	P_n	M_u	P_u	P_u/P_n	
PSC-F1	Construction	297.1	198.1	400.4	266.9	1.35	-
	Maximum load	468.4	312.3	654.7	436.5	1.40	Slip failure
PSC-F2		1328.6	885.8	1377.8	918.5	1.04	Flexural failure
RC-F3		1364.0	909.3	1370.4	913.6	1.00	Flexural failure

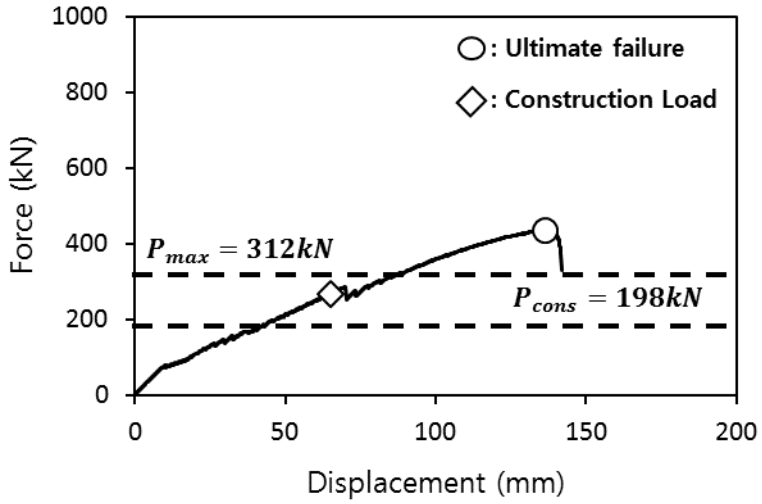

Figure 4-10 Load-Displacement relationship of PSC-F1

The initial stiffness was maintained as the load was applied, but the bolt slip occurred from the load of 70 kN. It was inevitable even though the bolt hole clearance was reduced to 1mm and the friction joint was applied. Lots of stiffness were lost with the bolt slip, and then the load increased with continuous slip.

It showed proper resistance in the construction load failure mode, which is 60% yield of top chord, and then it continues to resist the load without lateral buckling. The final strength was destroyed at 436.5 kN. During the fracture, the concrete was destroyed as the transverse buckling support plate was lifted up, and lateral buckling was slightly appeared.

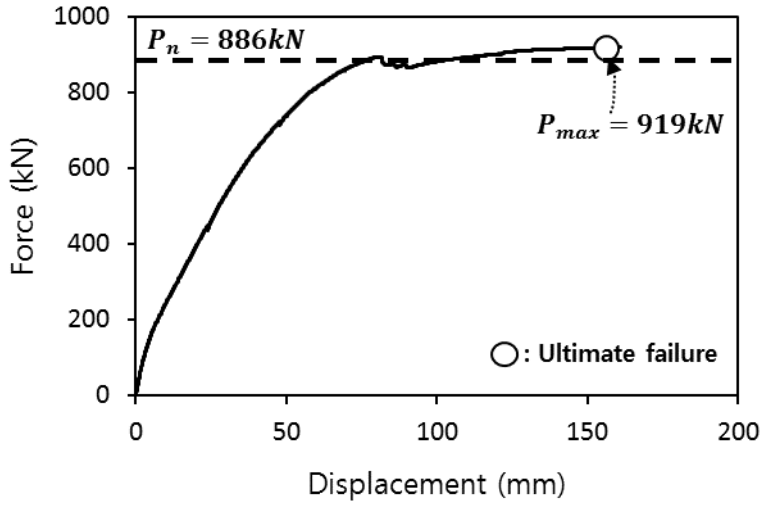

Figure 4-11 Load-Displacement relationship of PSC-F2

The PSC-F2 specimen is the permanent load section of PSC-F1. The first bending crack was found at 97 kN. After 230 kN, the bending cracks propagated to the upper section through the lower section. The first diagonal crack was found at the left side at 275 kN. However, after that, flexural cracks were more developed than diagonal cracks and horizontal cracks were hardly seen.

At 890 kN, concrete crushing started at the left loading point. Crushing occurred in 30 ~ 50mm thickness, and the load was slightly decreased, but then increased slightly. After showing a ductile behavior, after deflection of 150 mm, due to excessive deformation, the second-deep crushing occurred and the strength was completely lost.

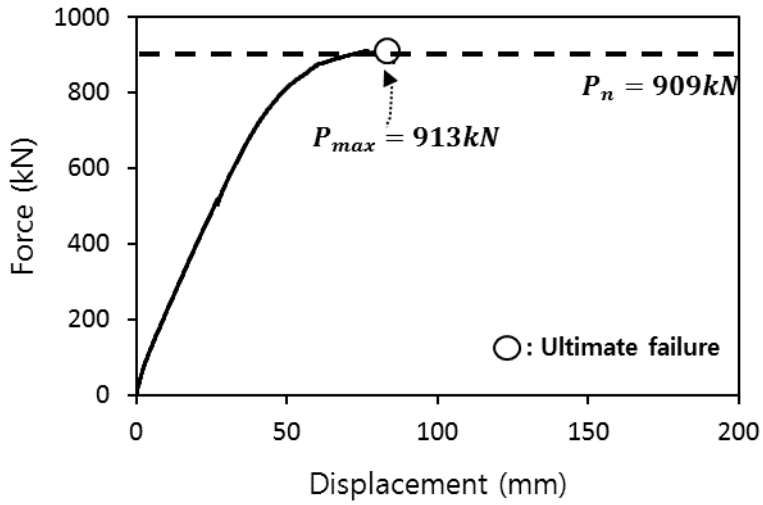

Figure 4-12 Load-Displacement relationship of RC-F3

In RC-F3 specimens, flexural cracks were found at 50 kN. After that, the flexural cracks propagate to the upper section through the lower section at 250kN tune. Thereafter, the flexural cracks developed more than the diagonal cracks, and horizontal cracks were hardly seen. At 880 kN, concrete crushing started at the left loading point and crushing spread. The load decreased after the maximum load of 913kN.

4.7.2 Comparison with proposed plastic moment equation

The Deseign equation will proposed in Chapter 6. The equation's objective is to calculate predicted strength of angle truss composite beam easily. The section in calculation is the same with RC-F3.

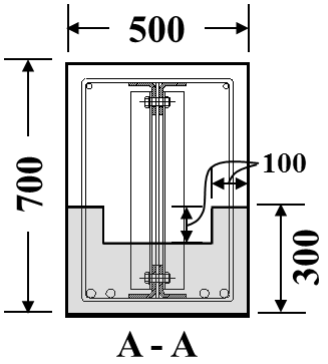

The variables are reinforcements ratio in the bottom. The experimental results were compared with those of the exact method and the simple method. The design equation was drawn based on the lower rebar ratio, and the experimental values are the test value of RC-F3.

The position of the neutral axis of the experimental results is larger than the value of the design equation assuming the plastic moment, which agrees well with the common sense. Also, the moment strength of the test results were in good agreement with those of the plastic moments.

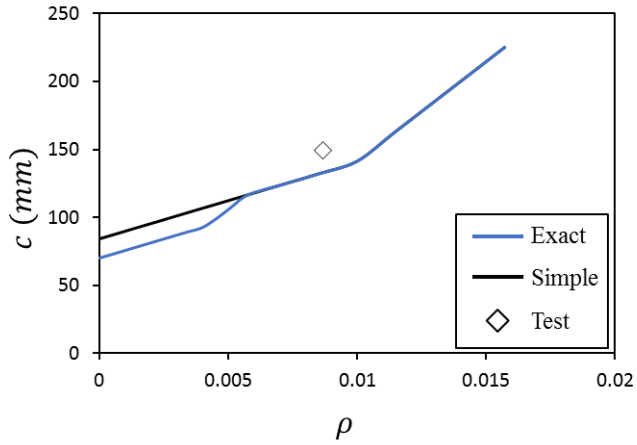

(a) Neutral axix depth

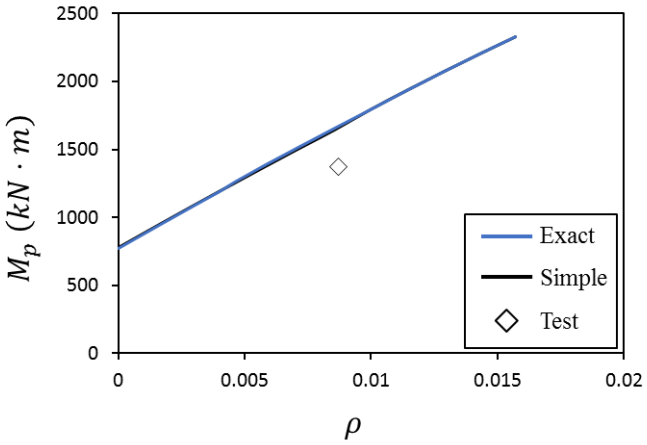

(b) Plastic moment

Figure 4-13 The comparison test results with proposed equation

4.8 Discussion

In this study, the bending performance of the angle truss composite beams was verified through experiments. The failure mode of the construction section (PSC-F1) was defined as the 60% yield of the top chord, and the failure mode of the ultimate section was predicted to be flexural failure. Therefore, the bending strength was evaluated by the monotonic loading test on the designed three beam specimens. The main results of this study are as follows.

1) In PSC-F1, a lateral buckling prevention plate was attached to prevent lateral torsional buckling. This is effective in preventing lateral torsional buckling until the maximum load is reached.

2) In the construction section using bolt-type angle truss, the bolt clearance was reduced to 1mm and slip-critical connections were used. Nevertheless, slip occurred at 30% of the target load (construction load) and the sitffness was lost.

3) Experimental results of PSC-F2 and RC-F3 well matched with the bending strength calculated by the strain compatibility method. Therefore, angle truss composite beam's flexural capacity can be determined by strain compatibility method.

Chapter 5. Shear Test for RC Angle Truss Composite Beams

5.1 Introduction

Angle truss composite beams composed of concrete, transverse reinforcements, and steel angle truss in shear components. The truss is located in the center of section to resist the construction loads. This member is defined as a encased composite member. The shear strength of encased composite member is specified in the AISC code provision. However, the equations proposed in the present code have few related studies.

The experiment was planned in order to evaluate the shear strength of angle truss composite beams which are a kind of encased composite beams. The test's objective is verifying the effect of shear contribution of the angle truss, which is added to nominal shear strength of reinforced concrete portion.

Experimental results showed that the test strength expressed 84 ~ 101% of predicted shear strength. The shear strength of the web members in angle truss are calculated in such a way that the transverse reinforcements were calculated. Because the angle truss webs are not continuous web, their shear behavior is similar to the transverse reinforcements not to I-shaped member's webs. The specimens without angle truss exhibited diagonal tension failure. However, the specimens with angle truss showed diagonal tension failure, shear bond failure, or combined failure. Shear bond failure caused due to insufficient bond strength at the surface between top angles and cover concrete.

From the test results, the shear strength increased largely due to encasement of angle truss. But in shear bond failure case, the shear strength of angle truss composite beams showed insufficient strength. In diagonal tension failure case, the shear strength is reached to the expected strength. Therefore, if the specimens have the sufficient bond strength, the angle truss composite beams show the expected strength, which is combined with concrete, steel, and transverse reinforcements. Lastly, the shear strength of angle truss composite bemas are proposed.

The history of ANSI/AISC 360 code provision

The Specification provides the generally applicable requirements for the design and construction of structural steel buildings and other structures. Both LRFD and ASD methods of design are incorporated. **Figure 5-1** shows the history of AISC codes.

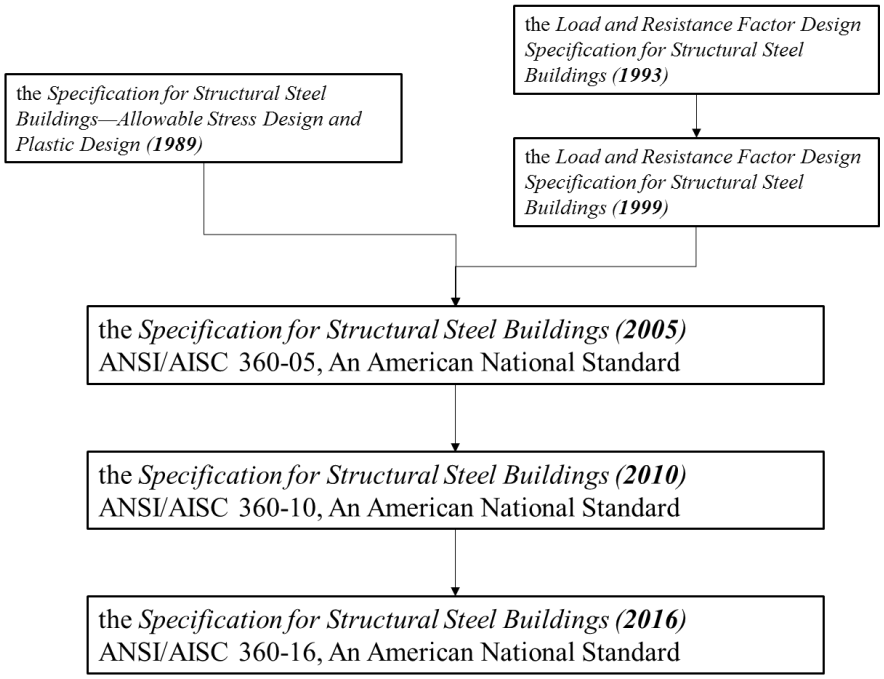

Figure 5-1 The history of ANSI/AISC 360 code provision

In the beginning, the AISC code proposed the design method both Allowable stress design (ASD) and Load and Resistance Factor Design (LRFD). Allowable stress design concept is calculating allowable stress of member with elastic analysis and use safety facor (Ω). and load and resistance factor design concept are calculating ultimate stress of member with inelastic analysis and use load combinations and strength reduction factor (ϕ).

In 2005, ASD design and LRFD design were united. the specification for structural steel building, ANSI/AISC 360-05 as an American national standard, was published.

The history of composite members' shear strength in AISC code

In ASD and LRFD code, the design shear strength of composite beams shall be determined by the shear strength of the steel web.

From ANSI/AISC 360-05, composite members were classified as axial, flexural, combined force members. The code defines shear strength of each type of composite members repectively. In axial members, shear strength of encased composite columns was defined as steel shear strength or reinforced concrete shear strength. So, shear strength was steel shear plus transverse reinforcement strength or reinforced concrete shear from ACI 318. And Filled composite columns' shear strength is defined shear strength of steel or reinforced concrete shear from ACI 318. In flexural members, shear strength of composite beams with shear connectors was steel web shear strength. And shear strength of encased and filled composite members was defined steel strength or reinforcement concrete strength.

In ANSI/AISC 360-10 and ANSI/AISC 360-16, shear strength of composite member is integrated in chapter I4. Because, there was no significant difference in the shear strength between each load conditions. The shear strength can be calculated in three ways which are collection of each member.

First is steel shear strength only, which can be used in simple use. Next is reinforced concrete shear strength according with ACI 318. The last is steel shear strength plus transverse reinforcement strength. And the code's commentary said that Though it would be logical to suggest provisions where both the contributions of the steel section and reinforced concrete are

superimposed, there is insufficient research. Overall changes are summarized in **Table 5-1**.

Table 5-1 The changes of the design shear strength equation in composite members

Code provsion	Classification of Composite members		Shear Strength
	Loading Condition	Section	
LRFD	Axial, Flexrual, Combined	Steel beam with shear connectors	$V_n = V_{web}$
ANSI/AISC 360-05	Axial, Flexrual, Combined	Filled composite members	$V_n = V_{steel} + V_{stirrup}$ or, $V_n = V_c + V_{stirrup}$
		Encased composite members	$V_n = V_{steel}$ or, $V_n = V_c + V_{stirrup}$
		Steel beam with shear connectors	$V_n = V_{steel}$
ANSI/AISC 360-10, ANSI/AISC 360-16	Axial, Flexrual, Combined	Filled composite members, Encased composite members, Steel beam with shear connectors	(a) $V_n = V_{steel}$ (b) $V_n = V_c + V_{stirrup}$ (c) $V_n = V_{steel} + V_{stirrup}$

5.2 Shear Strength of angle truss compsite beams

The shear strength of angle truss composite beams consists of concrete portion, shear reinforcements portion and angle truss portion. In this section, shear thory will be introduced and the design equation also be contained from ACI code provision. Because concrete and shear reinforcements are covered in ACI. And angle truss is also applied in the same code within encased condition.

Concrete shear strength

There are various theories for the shear strength of concrete. However, in this shear performance test, the shear strength was evaluated based on ACI standard in order for test objective.

From the shear theory, shearing stress can be determined by **Eq.(5-1)** in rectangular cross section.

$$\tau = \frac{VQ}{Ib} \tag{5-1}$$

$$Q = \int y\, dA \tag{5-2}$$

where V = applied shear force, Q = first moment of cross-sectional are above the level at which the shear stress is being evalulated (**Eq.(5-2)**), I = moment of inertia, and b = width.

But this equation is not proper to predict the shear stress in concrete. Because shear theory assumes elastic material unlike concrete. If the cracked section's Q, I are used, this equation can be applied.

To get consistent results, ACI code proposed the equation (**Eq.(5-3)**) whch is kind of experimental equation.

$$V_c = 0.17\lambda\sqrt{f_{ck}}b_w d \tag{5-3}$$

where λ = 1.0 for normal weight concrete, f_{ck} = concrete compressive strength, d = the effective depth.

If concrete has dual strength, the shear strength can be determined by using **Eq.(5-4).**

$$V_c = V_{c1} + V_{c2} = \frac{1}{6}\sqrt{f_{ck,1}}b_w d_1 + \frac{1}{6}\sqrt{f_{ck,2}}b_w d_2 \tag{5-4}$$

where $f_{ck,1}$ = the upper part concrete's compressive strength, $f_{ck,2}$ = the lower part's, d_1 = the total depth of upper concrete, and d_2 = the distance from lower part concrete's top surface to the centroid of longitudinal reinforcements. Varibles in **Eq.(5-4)** are displayed in **Figure 5-2.**

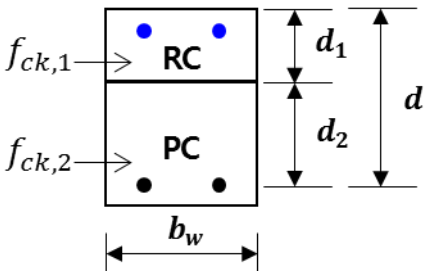

Figure 5-2 Concrete shear strength with dual concrete strength

Shear reinforcements and steel angle web shear strength

The shear strength of transverse reinforcements can be calculated by **Eq.(5-5).**

$$V_{stirrup} = \frac{A_v f_{yt} d}{s} \tag{5-5}$$

where A_v = the area of transverse reinforcements, f_{yt} = yield strength of transverse reinforcements, and s = spacing of transverse reinforcements. The **Eq.(5-5)** assumed the yield state of transverse reinforcements. After onset of diagonal crack on concrete, transverse reinforcements start elongation, which is caused by bond strength between reinforcement's rib and concrete.

Also, steel angle web member is going through the same procedure. There are two different things with transverse reinforcements. First one is that the web members consist of vertical members and diagonal members. The diagonal member is inclined at α angle with respect to the longitudinal direction. the second one is that steel members don't have direct bond strength to concrete, unlike transverse reinforcements, they are elongated by top and bottom chords' bearing strength, which is transferred by bolt shear connection. From the first one, the shear strength of steel angle web members is combined with two strengths of diagonal and vertical one. Because their shear strength is transferred by bolts, the maximum value of shear strength is bolt shear strength (or connection strength). So, the shear strength of steel angle web member can be determined by **Eq.(5-6)**, **(5-7).**

$$V_{vertical} = \frac{A_{sv} f_{ys} d}{s_a} \tag{5-6}$$

$$V_{diagonal} = \frac{A_{sd} f_{ys} (\sin\alpha + \cos\alpha) d}{s_a} \tag{5-7}$$

In the ACI standard, shear strength of reinforced concrete section is obtained by sum of shear strength of concrete and shear reinforcements. **Figure 5-3** indicates shear strength of reinforced concrete beam. When the reinforced beam was loaded, concrete resist the external shear strength. After diagonal crack was onset, transverse reinforcements yield.

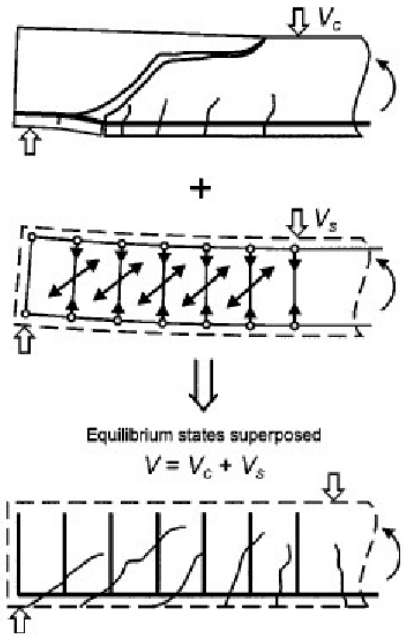

Figure 5-3 The shear strength of reinforced concrete beam

In the same way, the shear strength portion of angel truss composite member can be demonstrated by **Figure 5-4**.

(a) Concrete

(b) Shear reinforcements

(c) Steel web members

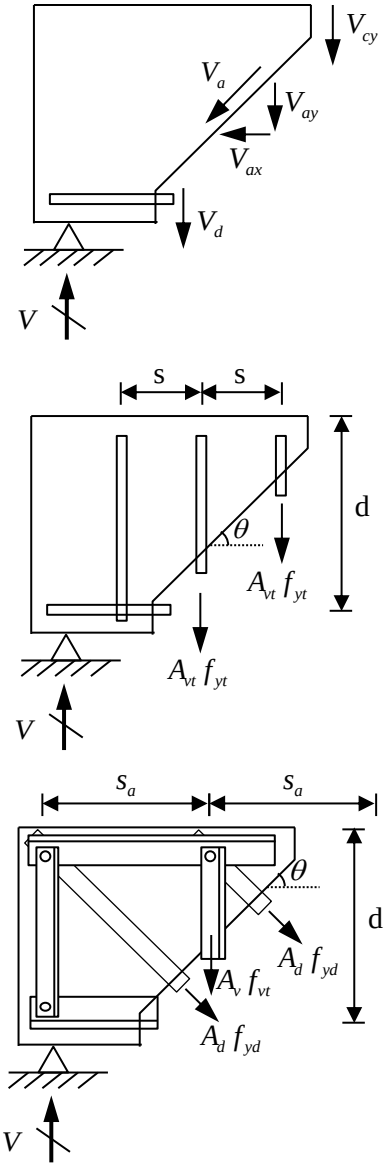

Figure 5-4 shear contribution of each portions

Therefore, the shear strength of angle truss composite beams can be calculated by **Eq.(5-8).**

$$V_n = V_c + V_{stirrup} + V_{steel} \tag{5-8}$$

where V_c = concrete shear strength, $V_{stirrup}$ = transverse reinforcements shear strength, and V_{steel} = steel web members shear strength ($= V_{vertical} + V_{diagonal}$).

Strictly speaking, the angle truss is not a part of member covered by AISC. Angle truss is a kind of steel joist. V_{steel} in the design equation proposed by AISC means actually V_{web}. I-shpaed member's web is continuous along the length. But angle truss's web is not. Also, since the web's behavior acts like transverse reinforcements, not a truss action. Therefore, it is reasonable to use stirrup equation, not a web shear equation.

5.3 Test Variables

The purpose of this experiment is to evaluate the shear performance of angle truss composite beam written in **Chapter 5.2**.

The main variables are presence of steel angle truss, presence of stirrup, and separation of concrete. Specimens' section and variables are listed in **Table 5-2** and **Figure 5-5**. To induce shear failure, diagonal members in truss were changed from 10T-plate in flexural test to 5T plate in shear test. Because the area of web members was a quite large to make shear failue.

Firstly, monotonic concrete shear specimes were designed. **RC-S1** was designed to evaluate the only concrete shear strength of general shear test specimen. **RC-S2** was designed to evaluate whether the shear strength of the angle truss is added to the shear strength of concrete by embedding an angle truss in the section of **RC-S1**. **RC-S3** was was designed to simultaneously arrange steel angle trusses and stirrups on the general RC section to see if the inner steel could contribute to the shear force when the actual angle composites were applied.

Next, Separate concrete strength shear test specimens were constructed. **RC-S4** has the same detail as **RC-S3**, but different concrete strengths of lower and upper concrete were placed separately. **RC-S5** is a concrete, stirrup and detachment test specimen similar to a conventional PC structure

The monotonic specimens' concrete strength was designed at 35 MPa. The separate concrete specimens are composed of dual concrete strength. The lower part concrete strength was designed at 60 MPa and the upper part concrete at 24 MPa to reflect the trend of high strength of concrete. The whole dimension of the beam section was 500 mm × 700 mm. and lower concrete depth is 250 mm and upper part depth is 450 mm total in 700 mm.

Table 5-2 Test variables of RC shear specimens

Specimen	Dimension (mm x mm)	f_{ck} (MPa)		Web member	
		Nominal (top / bot)	Material (top / bot)	Steel	Stirrup
RC-S1	500 x 700	35	54.2	-	-
RC-S2	500 x 700	35	54.2	Steel Angle Truss[1)]	-
RC-S3	500 x 700	35	54.2	Steel Angle Truss[1)]	D10@300mm
RC-S4	500 x 700	24 / 60	39.2 / 66.8	Steel Angle Truss[1)]	D10@300mm
RC-S5	500 x 700	24 / 60	39.2 / 66.8	-	D10@300mm

1) Steel Angle Truss = 2L-60x60-6T @ 600mm + PL-70-5mm @ 600mm
2) Web members are considered as transverse reinforcements

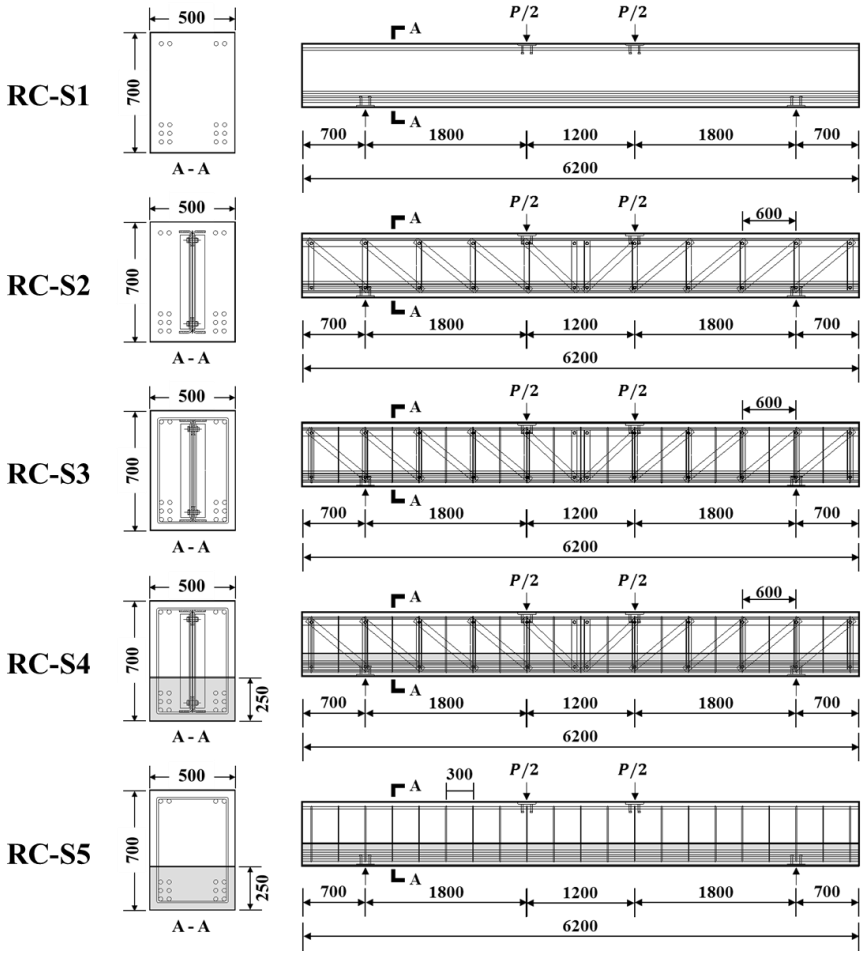

Figure 5-5 RC shear specimens section and side view

5.4 Specimens Design

Test specimens were designed to verify shear strength of angle truss composite beams, whici is composed of concrete, stirrups, and steel angle truss. Their flexural strength can be determined by method used in chapter.4. and their shear strength is calculated by summation of three components, which is also introduced in chapter 5.1. because this tests' objective is predictition of shear strength of angle truss composite beam, all specimens are designed at shear failure.

In the specimens, D25 bars (bar diameter d_b = 25.4 mm and yield strength f_y = 600 MPa) and D10 bars (bar diameter d_b = 10.7 mm and yield strength f_y = 400 MPa) were used for the longitudinal and transverse reinforcements, respectively. In steel angle truss, top and bottom chords are used in ATOS60 steel (yield strength f_y = 500 MPa, ultimate strength f_u = 600 MPa, elongation ε_u = 20 %). And web members are made of SS400 steel (yield strength f_y = 235 MPa, ultimate strength f_u = 400 MPa).

12-D25 tensile bars were placed in all specimens. D25 reinforcing bars were arranged in three layers of four. The stirrups were placed at 300 mm spacing. And steel angle truss is located in center of the section if present.

Specimens design results showed that the flexural strength was designed to be 1.55 to 2.75 times the shear strength.

Flexrual Capacity

RC-S1 and **RC-S5** specimens placed flexural reinforcements only. **RC-S2**, **RC-S3** and **RC-S4** specimens used both angle truss and flexural reinforcements.

In **RC-S1**, and **RC-S5**, they used only flexural reinforcements. So, their nominal bending sterngth can be obtained in the same way as general reinforced concrete beams by **Eq.(5-11).** In **RC-S2**, **RC-S3**, and **RC-S4**, when an angle truss is present, the bending strength is calculated assuming the perfectly bond of the angle truss by **Eq.(5-10)**. The specimens' flexural strengths are gathered in **Table 5-3**.

$$M_n = A_{sr} f_{yr} \left(d - \frac{a}{2} \right) \tag{5-9}$$

$$M_n = \left(A_{sr} f_{yr} + A_{sa} f_{ya} \right) \left(d - \frac{a}{2} \right) \tag{5-10}$$

Table 5-3 The specimens' neutral axis depth and flexural strength

Specimens	The depth of neutral axis	Nominal moment strength (kN·m)
RC-S1	227 mm	1898
RC-S2	235 mm	2407
RC-S3	235 mm	2407
RC-S4	292 mm	2272
RC-S5	290 mm	1756

Shear Capacity

Shear strength will be calculated by sum of concrete strength, shear reinforcement strength and web member strength. Concrete shear strength is designed by ACI 318. If dual concrete strengths are used, And web members are assumed to act like transverse reinforcements using **Eq.(5-3) ~ (5-8).**

Specimen design results is summarized in **Table 5-4**. V_m is the shear force causing nominal flexural strength. So, if V_m/V_n is greater than 1.0, that means the spcecimens will be failed in shear failure. All specimens were predicted shear failure.

Table 5-4 RC shear specimens design results

Specimen	Dimension	Shear strength (kN)				V_m	V_m/V_n
		V_c	V_{steel} [2)]	$V_{stirrup}$	V_n		
RC-S1	Rectangular Beam (500 × 700)	368.0	-	-	368.0	1054.4	2.87
RC-S2		368.0	440.5	-	808.5	1380.8	1.71
RC-S3		368.0	440.5	113.6	922.1	1380.8	1.50
RC-S4		337.0	440.5	113.6	891.1	1307.5	1.47
RC-S5		337.0	-	113.6	450.6	977.5	2.17

1) Steel Angle Truss = 2L-60x60-6T @ 600mm + PL-70-5mm(39.3deg.) @ 600mm
2) Web members are considered as transverse reinforcements

5.5 Test Method

The number of shear specimens is 5. Test setup was designed to perform shear test. The total length of the test specimen was 6.2 m. And the shear test was performed at 4 points test setup. 3000 kN capacity UTM (Universal Testing Machine) is used to perform the test. **Figure 5-6** shows the test setup for shear test. 2 points loading was applied using a 1.2 m span jig. The support condition was roller condition, which are located 700 mm apart from the end of the specimen. That is, the shear span is 1,800 mm and the effective depth of the test specimen is 600 mm, and the shear span ratio is $a/d = 3.0$ which means slender beam.

The experiment is controlled by displacement. The test speed was 0.03 mm/sec, and strain gauges were installed on the angled truss and inner reinforcement. Data measurements were taken every second. In the middle of the experiment, the experiment was stopped to draw cracks on the concrete, and then reloaded.

In order to measure the displacement, 5-LVDTs (The linear variable differential transformer) were installed at 600mm interval in the below part of the specimen. LVDTs were measured with bar.

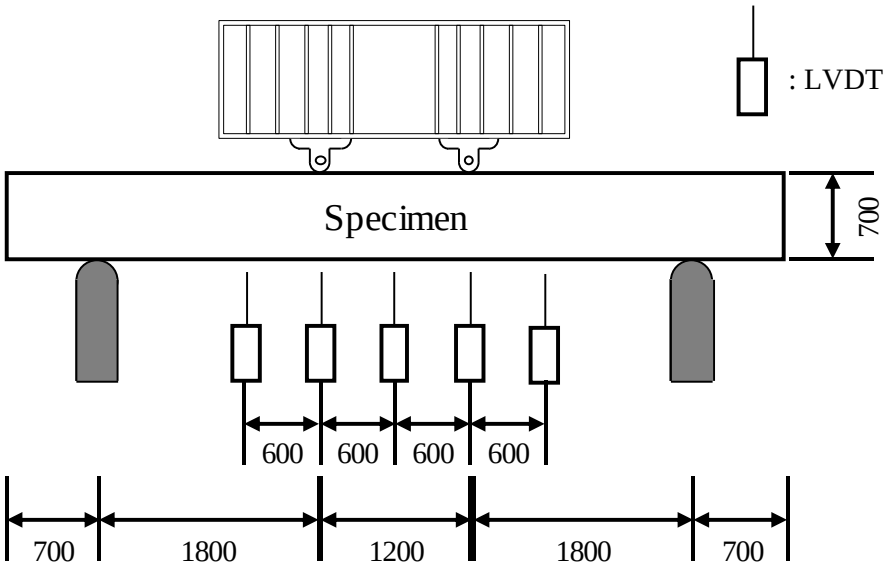

Figure 5-6 Shear test setup of angle truss composite beam

5.6 Test Results

5.6.1 Load-Displacment Relationships

All specimen both RC unified and RC composite section failed in diagonal tension failure, shear bond failure, or horizontal shear failure. The test results of RC shear specimens are summarized in **Table 5-5**. Normally, the strength of the specimen didn't exceed the expected strength. RC-S1 and RC-S2 were 6.0 %, 16 % less than expected strength, and RC-S3 showed the similar with expected strength. RC-S4 and RC-S5 were 1 ~ 2 % lower than expected strength.

Table 5-5 RC shear specimen test results

Speci-men	f_{ck} (MPa)		Shear strength (kN)			P_n	P_u	P_u/P_n	Failure modes
	Bot	Top	V_c	V_{steel}	$V_{stirrup}$				
RC-S1	54.2		368	0	0	735.9	691.6	0.94	DT
RC-S2	54.2		368	440	0	1616.9	1365.6	0.84	SB
RC-S3	54.2		368	440	130	1876.3	1887.0	1.01	DT
RC-S4	66.8	39.2	337	440	130	1814.5	1775.2	0.98	SB+DT
RC-S5	66.8	39.2	337	0	130	933.5	928.6	0.99	DT+HS

1) DT : Diagonal tension failure, SB : Shear bond failure, HS : Horizontal shear failure

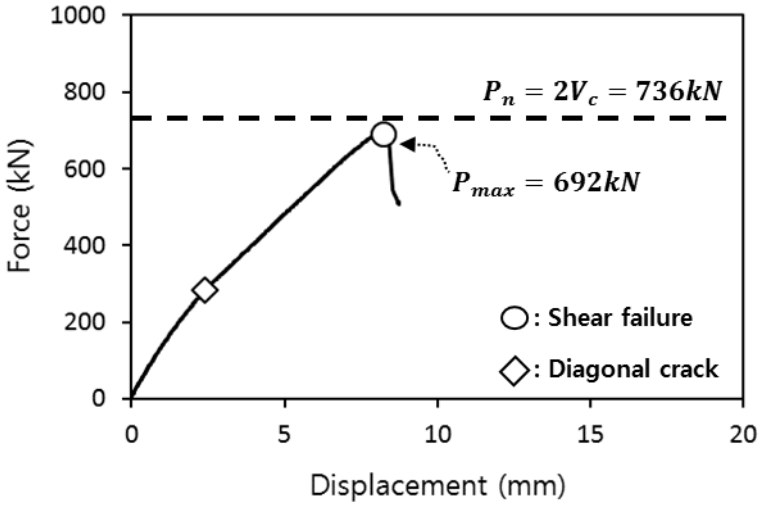

Figure 5-7 Load-displacement relationship of RC-S1

RC-S1 is monolithic RC shear beam without shear reinforcements. At 145 kN, flexural cracks began at center of the beam. Diagonal crack is firstly observed at $P = 283$ kN. It then spreads to the entire span as it develops into bending-shear cracks. As a result, shear failure occurred in RC-S1 due to brittle fracture at the right shear span at maximum load $P_u = 692$ kN (center deflection = 8.2 mm), and then the load-carrying capacity dropped sharply. The maximum load was 6 % lower than the nominal strength.

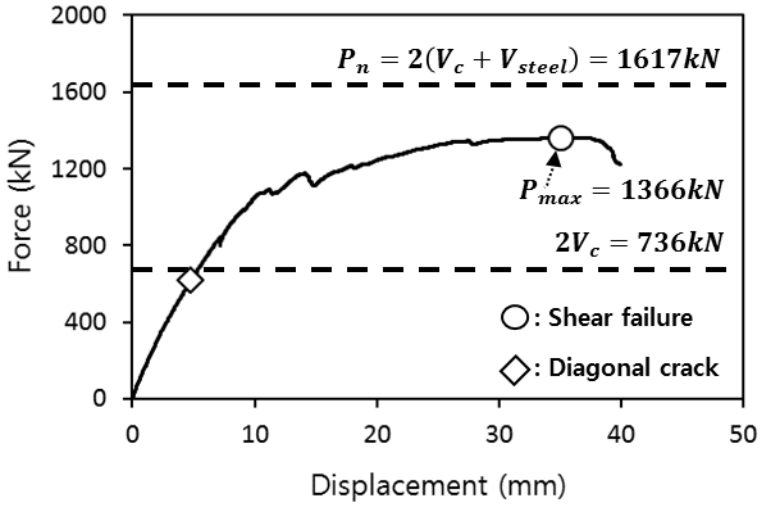

Figure 5-8 Load-displacement relationship of RC-S2

RC-S2 is casted in monolithic concrete. And encased angle truss is placed without shear reinforcements. The angle truss increases the flexural stiffness and shows a stiffer start compared to the RC-S1. A flexural crack occurred and the first diagonal crack was generated at the point of $P = 618$ kN. The diagonal cracks were then propagated to flexural-shear cracks. The flexural-shear cracks penetrated through the compression zone and the rigidity decreased sharply, but the acending second branch was observed due to the inner angle truss web members. As the cracks deepened in the right shear span, and Horizontal cracks were observed at the upper part of the specimen and the upper part was pushed outward. The location is the depth of top angle chord (50~60 mm depth from top surface). The maximum strength of the load $P = 1366$ kN (at 35.0 mm) was observed and then it was destroyed by the shear bond failure.

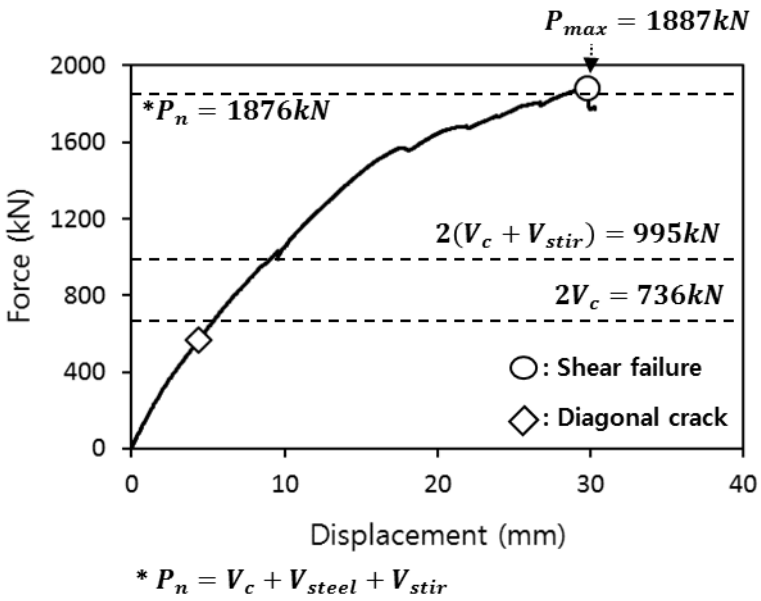

Figure 5-9 Load-displacement relationship of RC-S3

RC-S3 is monolithic concrete beam with angle truss and shear reinforcement. The initial stiffness was similar to that of RC-S2, and bending cracks occurred at $P = 190$ kN and dagonal cracks were observed for the first time at $P = 570$ kN. Diagonal cracks developed into flexural-shear cracks and penetrated into the tensile zone. The flexural-shear cracks then progressed to compression ($P = 1470$ kN) and the stiffness decreased. However, the shear contribution of the inner angle truss and shear reinforcement indicated an ascending second branch. After that, the load capacity was lost at the maximum strength $P = 1887$ kN (at 29.8 mm) which is a little more than predicted strength.

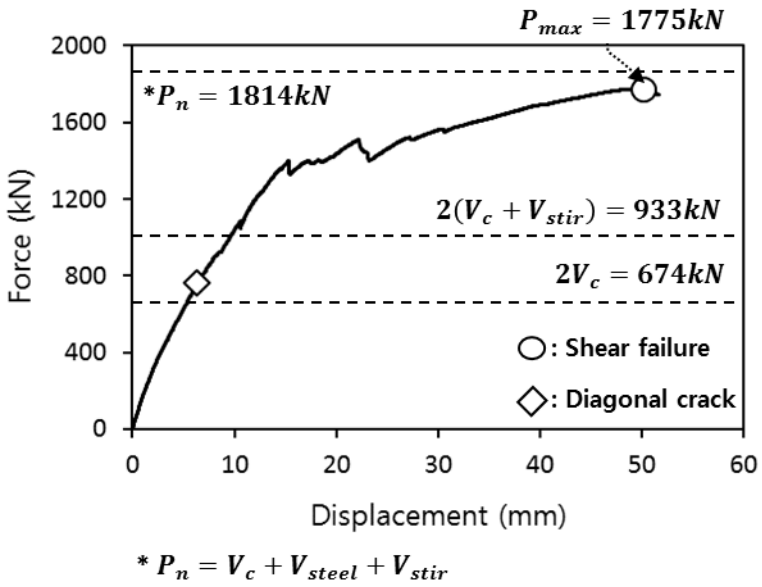

Figure 5-10 Load-displacement relationship of RC-S4

RC-S4 specimen was placed with dual concrete strength. High strength concrete was used for the bottom part and general strength concrete was used for the top part. Initial cracking occurred at $P = 219$ kN. At 430 kN, horizontal cracking began. Diagonal cracks occurred in the left side at $P = 760$ kN. At about $P = 920$ kN, the horizontal cracks greatly advanced. But horizontal slip is deterred by angle truss and shier reinforcement. At 1398 kN, the bending-shear cracks along with the hump progressed to compression and lost stiffness. Thereafter, an upper crack was formed at the upper side toward the point, and then a large crack was formed which led to the point passing through the upper part. At maximum strength $P = 1775$ kN (at 50.1 mm), shear bond failure occurred at maximum strength. Horizontal cracks in interface of concrete were observed, but slip was prevented by inner angle truss and transverse reinforcements.

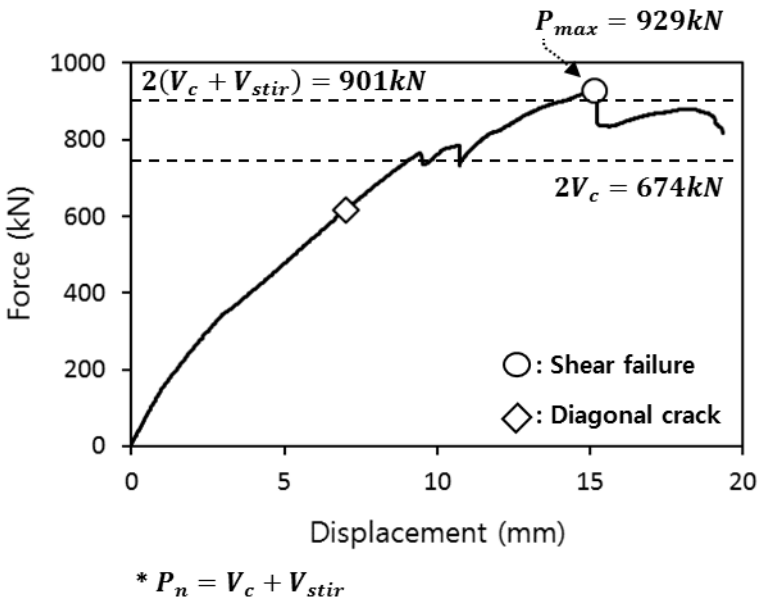

Figure 5-11 Load-displacement relationship of RC-S5

The RC-S5 is a specimen with detached specimens and shear reinforcements are placed inside without an angle truss. At $P = 180$ kN, bending cracks, $P = 350$ kN cracks climbed to the interface, horizontal cracking started from 400 kN. Diagonal cracks were found in horizontal cracks in the upper concrete, $P = 567$ kN, and horizontal cracks developed, but slips were not found. The diagonal crack penetrated the entire lower PC and the tension zone of the upper RC section while advancing to the flexure-shear crack. The slip was limited until the final failure, but the horizontal crack progressed. After the $P = 929$ kN was expressed at 15.1 mm, the experiment was terminated with decreasing load.

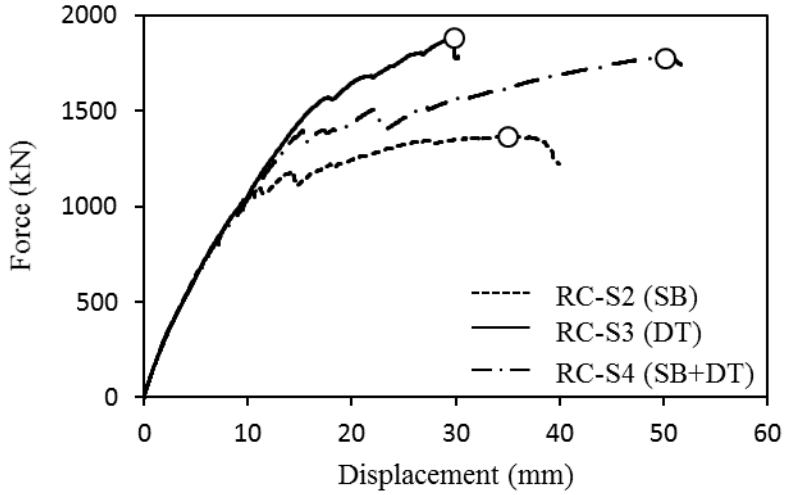

Figure 5-12 Load-displacement relationship of RC-S2, RC-S3, RC-S4

The load-displacement relationsip of RC-S2, RC-S3, and RC-S4 shear tests with angle truss plotted on a single scale in **Figure 5-12**. RC-S2 failed shear bond failure, RC-S4 showed shear bond failure and diagonal tension failure, RC-S3 destroyed by diagonal tension failure. The graph also shows that the initial bending stiffness almost coincides with the angles of the placed reinforced bars in the longtidutinal direction (concrete sterngths are slightly different) for all three specimens. In the case of RC-S2, the flexural stiffness was lost after onset of the shear bond, and it was finally destroyed, which is less than 16% of the expected strength. In the case of the RC-S4, the stiffness was maintained a little longer, but this is considered to be the role of shear stirrup. However, it can be seen that the shear bond is destroyed after the stiffness is lost. RC-S3 showed little shear bond failure, and it was found that the RC-S3 retained a nearly high level of rigidity until the end.

5.6.2 Failure Modes and Crack Patterns

Comparing the experimental results with the expected strength, RC-S3, RC-S4 and RC-S5 nearly reached the expected strength, but the results of RC-S1, and RC-S2 are below the expected strength. In the case of RC-S1, it can be concluded that early fracture occurred due to the uncertainty of concrete shear strength.

However, the failure of RC-S2 and RC-S4 was different. This is because the cracks of different shapes are found instead of the diagonal tensile fracture caused by the flexural-shear crack, which is a conventional shear failure mode.

Cracks and photographs of all shear test specimens are displayed in **Figure 5-13, Figure 5-14, Figure 5-15, Figure 5-16**, and **Figure 5-17.**

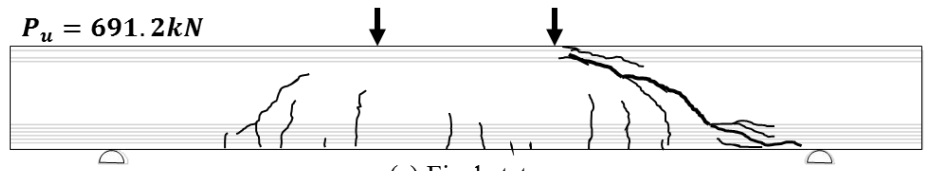

(a) Final state

(b) Picture at failure

Figure 5-13 Failure mode and crack pattern of RC-S1 specimen

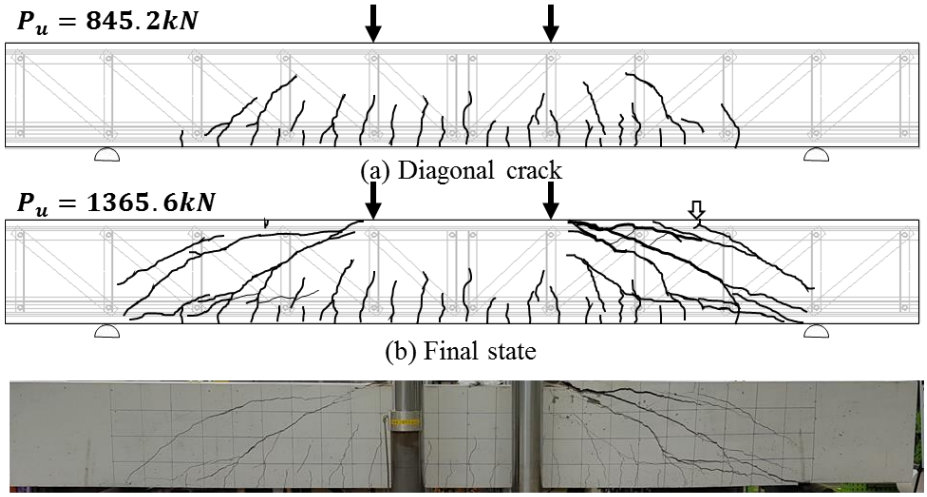

Figure 5-14 Failure mode and crack pattern of RC-S2 specimen

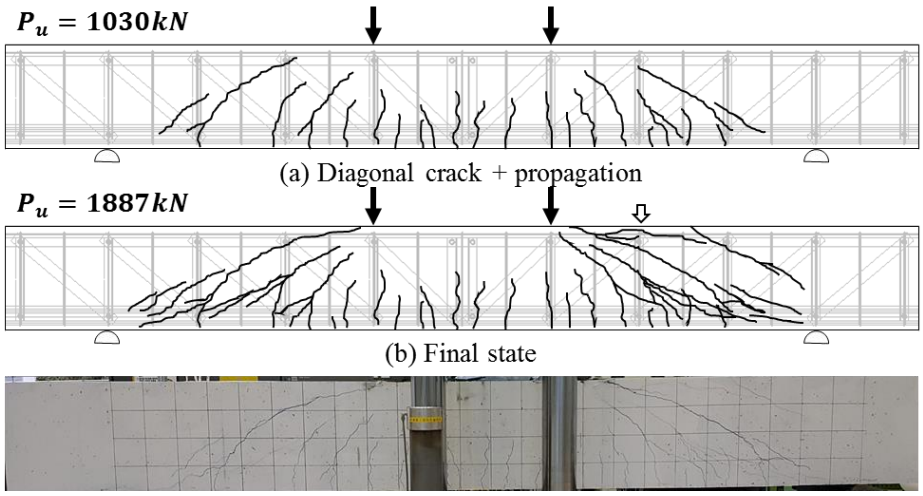

Figure 5-15 Failure mode and crack pattern of RC-S3 specimen

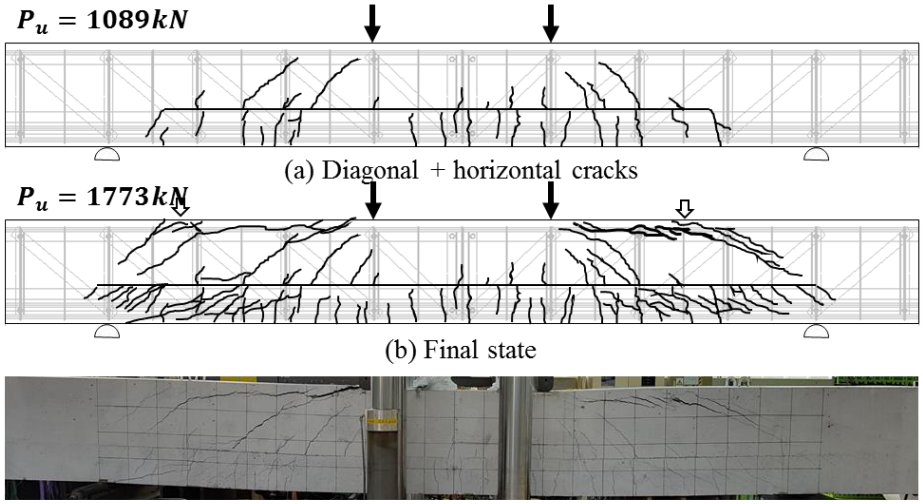

(a) Diagonal + horizontal cracks

(b) Final state

(c) Picture at final state

Figure 5-16 Failure mode and crack pattern of RC-S4 specimen

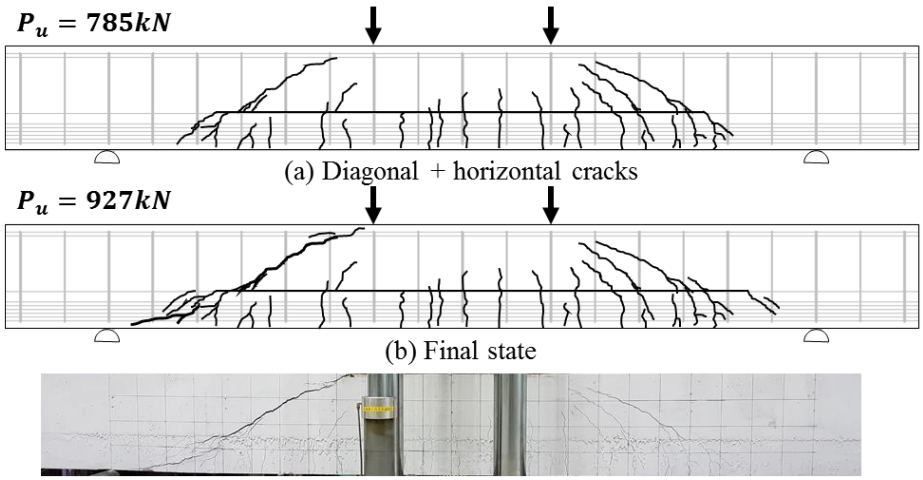

(a) Diagonal + horizontal cracks

(b) Final state

(c) Picture at final state

Figure 5-17 Failure mode and crack pattern of RC-S5 specimen

Unlike typical shear failure, horizontal shear bond failure due to the presence of angle trusses was found. This is caused by insufficient bond strength between top angle chords and upper concrete. **Figure 5-18** shows the potential sher nond failure plane. The witdh is reduced due to top chord angle's flange. Therefore, resistance width is changed from B to $(B - b_f)$.

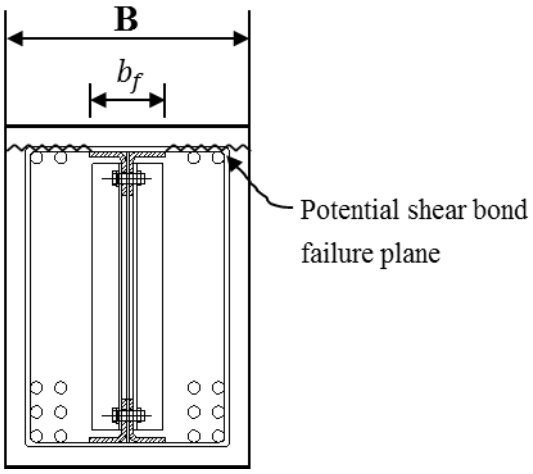

Figure 5-18 The potential shear bond failure plane

If the beam is under external shaer force, shear bond failure can be occured due to change of flexural compressive force at the potential shear bond failure plane.

Loov et al. proposed Eq.(5-11). This equation is verified various test results including Mattoct et al.

$$v_n = k\sqrt{\left(0.1+\rho_v f_y\right) f_c'} \le 0.25 f_c' \tag{5-11}$$

The above equation gives a conservative prediction of the experimental results. Basically, the k value is 0.5, but the additional level of safety for the monolithic construction is given as 0.6. The shear test specimens are casted monolithic in the potential bond failure plane. So, the value of k can be used as 0.6. In addition, when considering the configuration of the section, the contribution of shear reinforcement was ignored conservatively.

Using **Eq.(5-11)**, the V_{nh} of the test specimens can be calculated through the concept of the strength of the horizontal shear force. To use the concept of strength, the stress must be multiplied by the area, which is determined by the horizontal surface resisting area at that time **Eq.(5-12)** can be used.

$$V_{nh} = v_{nh} A_{ch} \tag{5-12}$$

where, $A_{ch} = \left(B - b_f\right) a$ and a is the shear span of test specimen.

In determining the demand horizontal shear force, V_{uh} was calculated by using $0.85 f_{ck}$, which is the concrete stress distribution assuming that the maximum bending strength has been reached. The calculation results are summarized in **Table 5-6**.

Table 5-6 Horizontal shear strength in shear specimens

	RC-S1	RC-S2	RC-S3	RC-S4	RC-S5
f_{ck} (MPa)	54.2	54.2	54.2	39.2	39.2
$\rho_v f_y$	0	0	0	0	0
v_{nh} (MPa)	1.397	1.397	1.397	1.188	1.188
V_{nh} (kN)	1257.2	867.4	867.4	737.7	1069.1
V_{uh} (kN)	1151.8	1151.8	1151.8	833.0	833.0
V_{nh}/V_{uh}	1.09	0.75	0.75	0.89	1.28

ρ_v is considered as 0 due to conservative assement

If V_{nh}/V_{uh} is greater than 1.0, it is safe for horizontal shear

Since RC-S1 and RC-S5 are general RC shear tests without angle trusses, the effective width of the concrete is equal to the overall width of the beam. And horizontal shear strength is sufficient.

However, RC-S2, RC-S3, and RC-S4 were found to lack the horizontal shear force. This is consistent with the observation that horizontal shear failure was observed in the test results except RC-S3.

5.6.3 Strain gauge measurement

Strain gauges were attached to the stirrups and the angle truss web member of all shear specimens except for the RC-S1 shear specimen which is unreinforced. In angle truss web, strain gauges are attached 4 to each side. And in stirrups, strain gauges are attached 3 to each side. Strain was measured every second in the progress of the experiment.

Figure 5-19 ~ Figure 5-22 shows the location of strain gauges and the value measured in each state.

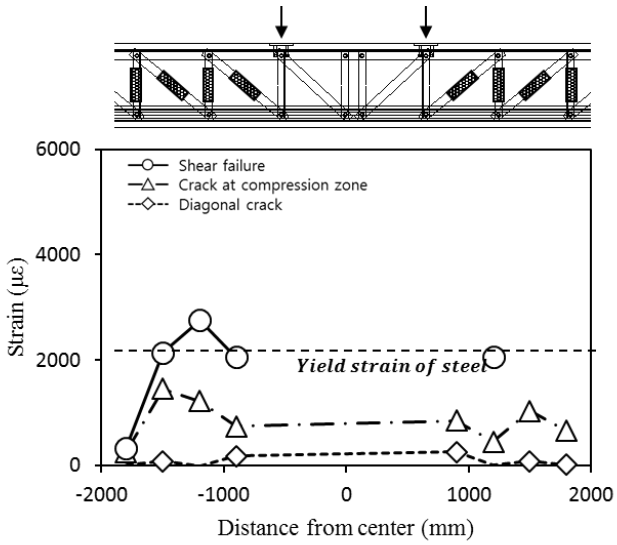

Figure 5-19 Strain gauge measurements in RC-S2

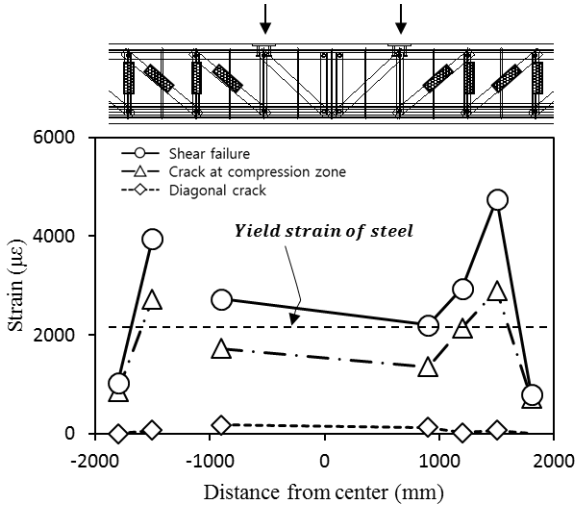

(a) Angle truss web strain

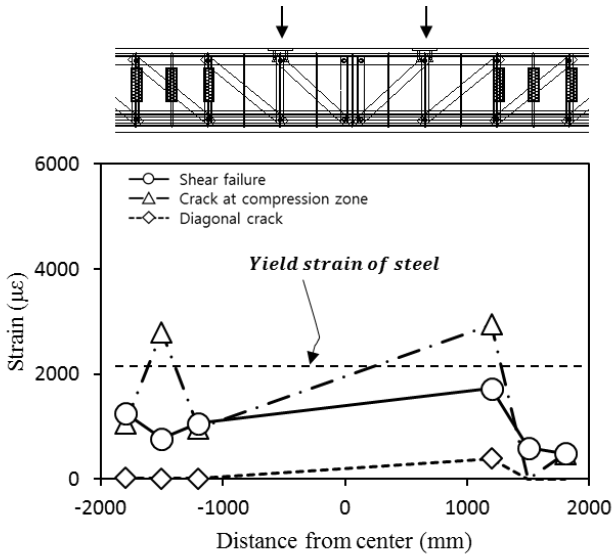

(b) Stirrups strain

Figure 5-20 Strain gauge measurements in RC-S3

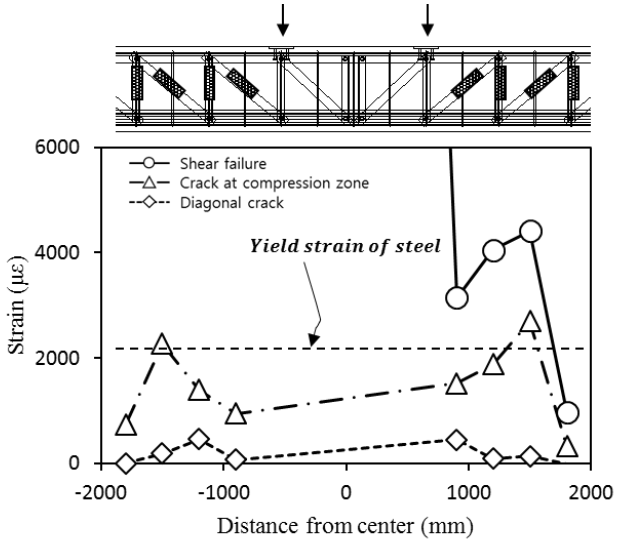

(a) Angle truss web stran

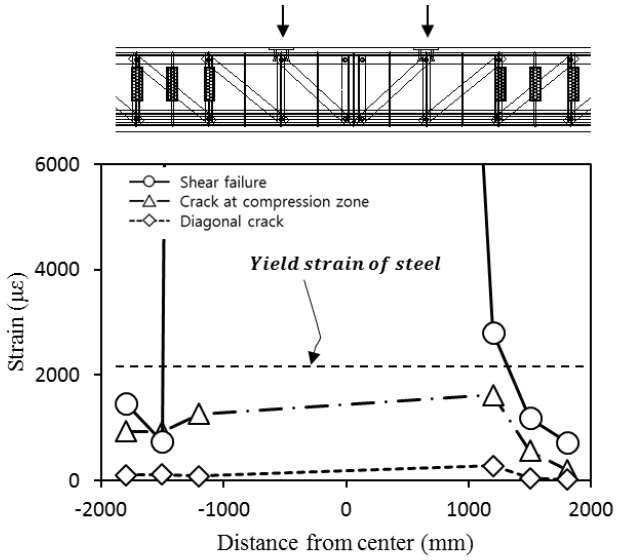

(b) Stirrups strain

Figure 5-21 Strain gauge measurements in RC-S4

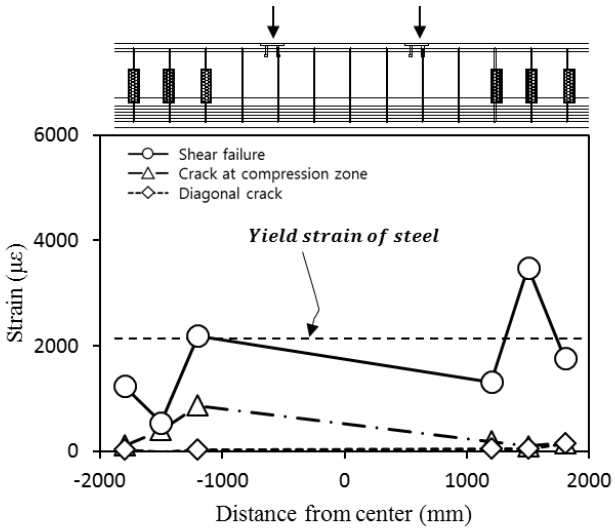

Figure 5-22 Strain gauge measurements in RC-S5

The strain of web member and stirrup was yielded in the following order as a whole. The deformation of the diagonal member at the center side of the load point starts immediately after the cracking of the signatures. At the same time, deformation of the stirrup and the vertical member increases sharply. Then, the outer frame and stirrup are deformed. Deformation was limited in the case of the outer vertical member, and deformation in the large vertical member was more deformed than in the stirrup. It was judged that this was arranged close to the perpendicular to the sinus. Even after the final destruction, we could see that the web of the inner angle was more deformed than the stirrup.

5.6.4 Shear contribution of steel web member

The web members of angle truss embedded in concrete act similar to that of shear reinforcement after the diagonal crack of concrete. Its model is shown by **Figure 5-23**.

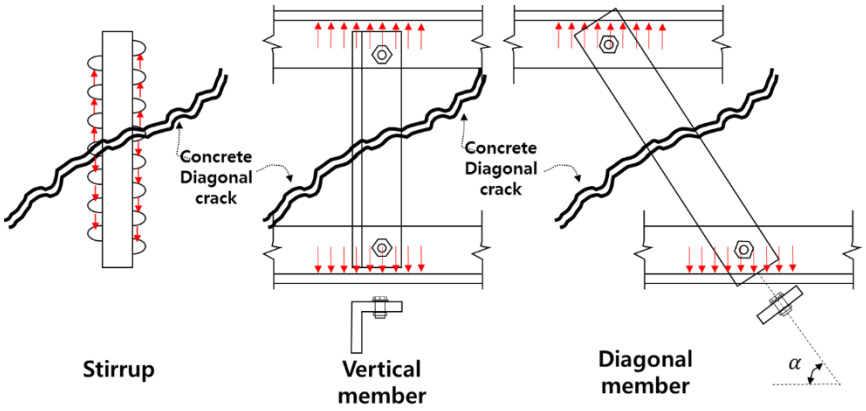

Figure 5-23 shear contribution of stirrup and steel web members

In the case of stirrups, the load is transmitted directly through the ribs attached to the reinforcing bars. However, the vertical members and diagonal members of the angle truss are elongated through the upper and lower bearing force, and thus the shear strength is developed. Here, the bolt is connected, which will be set as the upper limit of the shear strength of web members. The equation is expressed as follows.

The three components of shear reinforcement were analyzed.

(1) Transverse reinforcement

The stirrup can be yield by the direct bearing with rib. **Eq.(2-10)** can be used.

$$V_{stirrup} = \frac{A_v f_{yt} d}{s} \tag{2-10}$$

(2) Vertical member

The vertical member is elongated by bearing force. And its limitation is the bolt's shear strength. Therefore, the bolt's shear strength is the maximum value of shear capacity. **Eq.(5-13)** is proposed.

$$V_{vertical} = \frac{A_{sv} f_{ys} d}{s} \le R_{n,v} \tag{5-13}$$

(3) Diagonal member

Diagonal member is the same with vertical member using **Eq.(5-14)**.

$$V_{diagonal} = \frac{V_{d,1}\left(\sin\alpha + \cos\alpha\right) d}{s} \le R_{n,d} \tag{5-14}$$

5.7 Discussion

In this study, the bending performance of the angle truss composite beams was verified through experiments. The failure mode of the construction section (PSC-F1) was defined as the 60% yield of the top chord, and the failure mode of the ultimate section was predicted to be flexural failure. Therefore, the bending strength was evaluated by the monotonic loading test on the designed three beam specimens. The main results of this study are as follows.

4) In PSC-F1, a lateral buckling prevention plate was attached to prevent lateral torsional buckling. This is effective in preventing lateral torsional buckling until the maximum load is reached.

5) In the construction section using bolt-type angle truss, the bolt clearance was reduced to 1mm and slip-critical connections were used. Nevertheless, slip occurred at 30% of the target load (construction load) and the sitffness was lost.

6) Experimental results of PSC-F2 and RC-F3 well matched with the bending strength calculated by the strain compatibility method. Therefore, angle truss composite beam's flexural capacity can be determined by strain compatibility method.

Chapter 6. The Structural Capacity of Angle Truss Composite Beams

6.1 Introduction

From previous chapters, angle truss composite beams's structural capacity was investigated. There are proposed equations to evaluate the structural performance of the angle truss composite beam based on the bending test and the shear test.

In case of flexural capacity, it is divided into a construction load section and a permanent load section. Construction section's failure mode is defined as 60% yield of top chords. Because only top angle chords resist the compressive force for bending moment. Ultimate section's failure mode is that compressive strain of top fiber concrete is 0.003, which is the same with conventional reinforced concrete beam. For the convenience of calculation, plastic stress distribution method can be used, which is introducted in **Chapter 6.3**. The exact method to consider bolt's hole and the simple method to nelect bolt's hole are presented and compared.

In case of shear performance, the web material of the angle truss is directly inserted into the shear strength according to the test results, and the upper limit value of the web member's shear strength is the bolt shear strength.

6.2 Construction Section Design

The section of the angle truss composite beam is the cross section in which the steel angle truss is embedded in the center and the lower section is casted in the precast concrete. It is assumed that the failure mode of construction section is 60% yield of the top chord, and it is confirmed with test results in **Chapter 4**. To help the angle truss composite beam design easily, this chapter will propose the method to obtain the bending strength of construction section.

Figure 6-1(a) shows the construction section of angel truss composite beam. To reach the failure mode, the compressive strain at the top is $0.6\varepsilon_{ya}$. And the strain distribution will be distributed linearly due to the assumption that plane remains plane. And in the case of prestressed beam, strain distribution shows the stepped change due to the prestressed force (**Figure 6-1(b)**).

From the strain distribution, stress of each member is also determined by the Hooke's law. On the tensile side, strands, rebars, and bottom chords cause tensile forces, whereas on the compressive side, only the top chords resist compressive force. From the force equilibrium, the magnitude of the tensile force and the compressive force should be the same. And moment arm can be considered as jd. Therefore, the moment strength can be calculated as **Eq. (6-1)**.

$$M_{n,c} = C(jd) = A_a F_{ya} jd \tag{6-1}$$

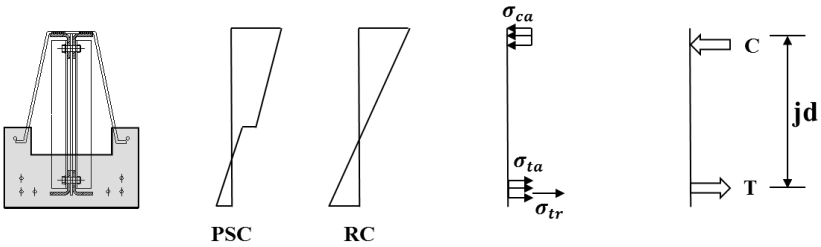

(a) Section (b) Strain distribution (c) Stress distribution (d) Resultant forces

Figure 6-1 Construction section of angle truss composite beam

From the section analysis, jd can be the exact effective depth of the section, or simply use 0.8h.

Through the above process, the moment strength of the construction section is determined. And it can be compared with the required strength by a given design condition. To provide the proper bending capacity, the size of the top angle can be varied. It caused by the fact that only top chords resist the compressive force.

6.3 Flexural capacity of Ultimate State

Angle truss composite beam is a kind of encased composite members, and the nominal moment of the encased composite members proposed by AISC can be obtained by two methods. The first one is plasitc strain distribution method and the second one is strain compatibility method. The reason why plastic moment is important here is that it can help easy design by determining the plastic moment by the hand calculations from the field engineer. Therefore, this section will introduce two methods to calculate plastic moment in angle truss composite beams and compare the exact method and the simple method to obtain the plastic moment. Because the cutback of steel angle area due to the bolt hole in the double angle, which is reflected in the exact method. And the simple method ignores the bolt hole as no presence by combining the area under the bolt hole to upper angle.

As a result, when the neutral axis is on the web of the double angle, there is a difference in neutral axix depth, c value estimation between the two methods. However, since the web contributes little to the bending strength, there is little difference in moment capacity between the two methods.

The sections and variables used in two methods are illustrated in **Figure 6-2**.

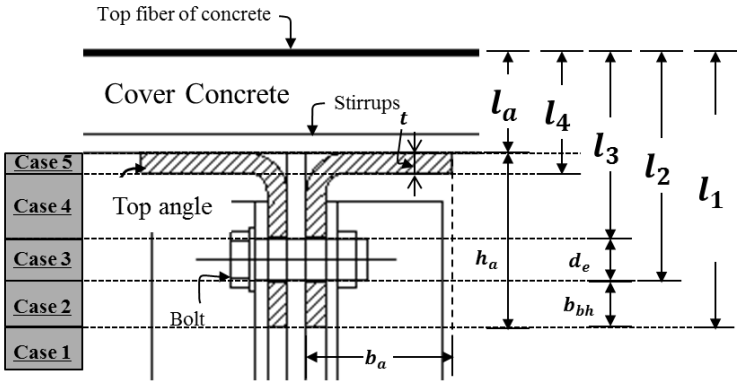

l_a : the distance from top fiber of concrete to top angle's upper surface
l_1 : the distance from top fiber of concrete to top angle's lower surface
b_a : the width of angle
h_a : the height of angle
b_{bh} : the length of angle below bolt hole
t : thickness of angle
d_e : bolt hole's diameter

(a) Conditions and variables of exact plastic moment

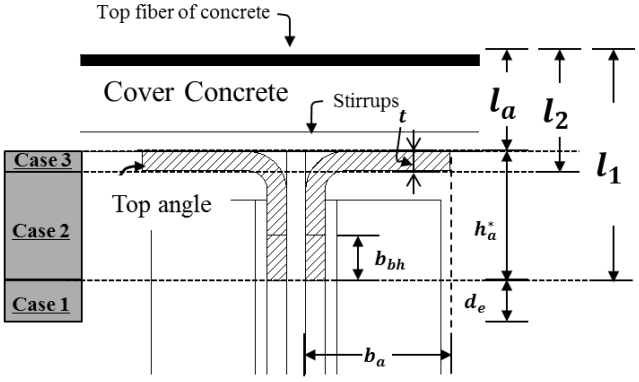

l_a : the distance from top fiber of concrete to top angle's upper surface
l_1 : the distance from top fiber of concrete to top angle's lower surface
b_a : the width of angle
h_a : the height of angle
h_a^* : the changed height of angle ($h_a^* = h_a - d_e$)
b_{bh} : the length of angle below bolt hole
t : thickness of angle
d_e : bolt hole's diameter

(b) Conditions and variables of simple plastic moment

Figure 6-2 Design condition to calculate plastic moment

Bases of calculation

1. Sign convention is that compression is positive, and tension is negative.

2. Equivalent stress block concept is used. Concrete stress is $0.85 f_{ck}$`, and β_1 is also used.

3. Top rebars and bottom rebars are distinguished.

4. Top angles and bottom angles are the same.

5. In Case 1, All area of top angles is in compression. $(c > l_1)$

6. In Case 2~5, Some area of top angles is in compression, and the other is in tension. $(l_a < c < l_a)$

In any cases, concrete and top rebar are in compression, and bottom rebar and bottom angles are in tension.

Exact Plastic Moment

Before calculation of exact platic moment, some calculation bases are required, which are already presented. And the cases were divided according to the position of the neutral axis (below the angles, in the angle's web, in the angle's flange). The case that the location of the neutral axis is above the angles are not considered due to the unrealistic.

Simple Plastic Moment

The simple method represented in **Figure 6-2(a)**. the figure indicated that removing bolt hole and combined upper part with lower part in angle. The basic calculation procedure is the same with the exact plastic moment. The different thing is that there is no bolt hole in simple method. Therefore, the number of cases reduced from 5 to 3. Only 3 cases will be considered. And its results are very similar to exact method. Because, angle's web contribution to bending moment is low due to small area and location.

Table 6-1 and **Table 6-2** indicate the cases to calculate moment capacity of each method. The procedure of precise calculation is presented in **Appendix A (exact method)** and **Appendix B (simple method)**. And in this chapter, only the results can be showed in **Table 6-3**, and **Table 6-4**. The results consist of the neutral axis depth, locations of centroid to be able to calculate bending moment.

Table 6-1 The cases divided depending on the neutral axis in exact method

Cases	Conditions	Location of neutral axis
Case 1	$c > l_1$	Below top angle
Case 2	$l_2 < c < l_1$	In angle's web
Case 3	$l_3 < c < l_2$	In angle's web
Case 4	$l_4 < c < l_3$	In angle's web
Case 5	$l_a < c < l_4$	In angle's flange

Table 6-2 The cases divided depending on the neutral axis in simple method

Cases	Conditions	Location of neutral axis
Case 1	$c > l_1$	Below top angle
Case 2	$l_2 < c < l_1$	In angle's web
Case 3	$l_a < c < l_4$	In angle's flange

Table 6-3 The calculation of neutral axis depth and the centroids of angle in exact plastic moment

Location of c		c	$\bar{y}_c$	$\bar{y}_t$
Below angle	Case1	$-\frac{C_a + C_r + T_a + T_r}{0.85 f_{ck} \beta_1 b}$	$\left(\frac{t}{A_{a1}}\right)\left(b_{uh}\left(\frac{b_{uh}}{2}+r\right)+b_{bh}\left(\frac{b_{bh}}{2}+d_e+b_{uh}+r\right)+0.363ur\right)$	
In angle's web	Case2	$\frac{4l_1 t F_{ya} - C_r - T_r}{0.85 f_{ck} \beta_1 b + 4t F_{ya}}$	$\left(\frac{t}{A_{a1}-y^* t}\right)\left(b_{uh}\left(\frac{b_{uh}}{2}+r\right)+y_2\left(\frac{y_2}{2}+d_e+b_{uh}+r\right)+0.363ur\right)$	$c+\frac{y^*}{2}$
	Case3	$-\frac{C_{ta} + C_r + T_{ta} + T_a + T_r}{0.85 f_{ck} \beta_1 b}$	$\left(\frac{t}{A_{a1}-b_{bh}t}\right)\left(b_{uh}\left(\frac{b_{uh}}{2}+r\right)+0.363ur\right)$	$l_2+\frac{b_{bh}}{2}$
	Case4	$\frac{4b_{bh} t F_{ya} + 4l_3 t F_{ya} - C_r - T_r}{0.85 f_{ck} \beta_1 b + 4t F_{ya}}$	$\left(\frac{t}{A_{a1}-b_{bh}t-y^* t}\right)\left(b_{uh}\left(\frac{b_{uh}}{2}+r\right)+y_4\left(\frac{y_4}{2}+r\right)+0.363ur\right)$	$c+\frac{y^*+b_{bh}}{2}+d_e$
In angle's flange	Case5	$\frac{2b_a l_a F_{ya} - C_r - 2T_a - T_r}{0.85 f_{ck} \beta_1 b + 2b_a F_{ya}}$	$l_a+\frac{c-l_a}{2}$	$\left(\frac{A_1}{A_{a1}}\right)\left(c+\frac{y^*}{2}\right)+\left(\frac{A_2}{A_{a1}}\right)\left(c+y^*+\frac{h_a-t}{2}\right)$

c is the neutral axis depth

$\bar{y}_c$ is the centroid of top angles in compression

$\bar{y}_t$ is the centroid of top angles in tension

Detail calculations are being presented.

Table 6-4 The calculation of neutral axis depth and the centroids of angle in simple plastic moment

Location of c		c	$\bar{y}_c$	$\bar{y}_t$
Below angle	Case1	$-\frac{C_a + C_r + T_a + T_r}{0.85 f_{ck} \beta_1 b}$	$\left(\frac{t}{A_{a1}}\right)\left((b_{uh} + b_{bh})\left(\frac{b_{uh} + b_{bh}}{2} + r\right) + 0.363ur\right)$	
In angle's web	Case2	$\frac{4l_1 t F_{ya} - C_r - T_r}{0.85 f_{ck} \beta_1 b + 4t F_{ya}}$	$\left(\frac{t}{A_{a1} - y^* t}\right)\left(y_2\left(\frac{y_2}{2} + r\right) + 0.363ur\right)$	$c + \frac{y^*}{2}$
In angle's flange	Case3	$\frac{2b_a l_a F_{ya} - C_r - 2T_a - T_r}{0.85 f_{ck} \beta_1 b + 2b_a F_{ya}}$	$l_a + \frac{c - l_a}{2}$	$\left(\frac{A_1}{A_{a1}}\right)\left(c + \frac{y^*}{2}\right) + \left(\frac{A_2}{A_{a1}}\right)\left(c + y^* + \frac{h_a - t}{2}\right)$

c is the neutral axis depth

$\bar{y}_c$ is the centroid of top angles in compression

$\bar{y}_t$ is the centroid of top angles in tension

Detail calculations are being presented.

Comparison of two methods

Two methods which is the calculation of plastic method in angle truss composite beams were introduced. This section's objective is comparison of two methods in order to verify and check the difference.

As the written, the different thing in two methods is how to dispose the bolt hole. Exact method calculates the same way in reality. However, simple method considered that there is no bolt hole in angle section. This is well explained in **Figure 6-2**.

The neutral axis's variation and the bending moment's variation is presented with respect to bottom rebar ratio in **Figure 6-3**. From the figure, there was a difference when the neutral axis is in angle's web (Case 2,3,4). In Case 2,3,4, the neutral axis depth shows the gap due to the presence of bolt hole. But, the plastic moment indicates little difference between two methods.

From the results, it is conclude that the simple method can be used in replace of the exact method to calculate plastic moment of angle truss composite beam.

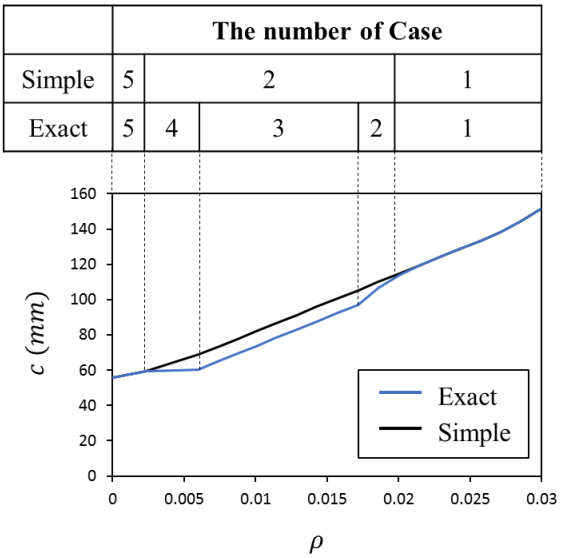

(a) The variation of neutral axis depth

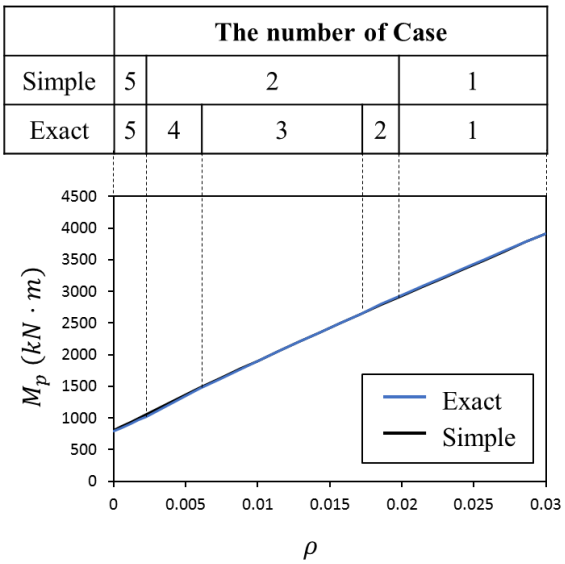

(b) The variation of plastic moment

Figure 6-3 The comparison of the two methods with respect to bottom rebar ratio

6.4 Shear Capacity of Ultimate State

The shear performance of the angle truss composite beams consists of three parts. First one is shear strength of concrete, second one is shear strength of trainsverse reinforcements, and the third one is the shear strength of angle trusses embedded inside. From the test results, it is also necessary to check the horizontal shear strength between the angle face and the concrete face at the top. The shear bond failure should be deterred because it is unwilling failure mode. The angle truss composite beam's shear strength can be calculated by **Eq.(6-2)**.

$$V_n = V_c + V_{stirrup} + V_{steel} \tag{6-2}$$

where, V_c = concrete shear strength, $V_{stirrup}$ = transverse reinforcement's shear strength, and V_{steel} = the angle truss web member's shear strength.

1) Concrete shear strength (V_c)

From ACI code provision, concrete shear strength can be determined by **Eq.(6-3).**

$$V_c = \frac{1}{6}\sqrt{f_{ck}}\, b_w d \tag{6-3}$$

2) Transvers reinforcement's shear strength ($V_{stirrup}$)

Also, ACI code provision is used by **Eq.(6-4)(6-5).**

$$V_{stirrup} = \frac{A_v f_{yt} d}{s} \tag{6-4}$$

If inclined stirrup is used,

$$V_{stirrup} = \frac{A_v f_{yt} (\sin\alpha + \cos\alpha) d}{s} \tag{6-5}$$

3) Angle truss web members' shear strength

Calculate the shear strength by replacing the web member area of the angle truss with the stirrup. The upper limit of the shear strength of each member at this time is calculated as the shear strength of the connecting brazing material. Finally, angle truss composite beam's shear strength can be calculated by **Eq.(6-6)**.

$$V_{steel} = V_{vertical} + V_{diagonal} \tag{6-6}$$

where,

$$V_{vertical} = \frac{A_{sv} f_{ys} d}{s} \le R_{n,v} \tag{6-7}$$

$$V_{diagonal} = \frac{V_{d,1} (\sin\alpha + \cos\alpha) d}{s} \le R_{n,d} \tag{6-8}$$

Chapter 7. Concluding Remarks

However, further study is required for the section details due to the occurrence of slip at bolted connections.

1) From flexural test results of angle truss composite beams, the proposed bond strength equation is well fitted with test results. Using the equation, the steel angle and the concrete showed complete adhesion behavior. Therefore, the bending strength can be calculated by applying the strain compatibility method.

2) From shear test results of angle truss composite beams, the shear force contributions of the three elements constituting the composite section were investigated. These are concrete, shear reinforcement, and angle truss web member. It was confirmed that the shear strength of the composite beams varied according to the presence or absence of each element. Therefore, shear strength of composite section can be calculated by sum of three elements.

3) To calculated angle truss web member's shear resistance, yield state is assumed. That is not guaranted under various conditions, so the strength of web member should be limited to certain point. And that is a shear strength of connector. In the case of an angle truss composite beam, the shear strength of the bolt is.

References

[1] AISC Committee on Specifications. (2010). *Specification for Structural Steel Buildings*. Americal Institute of Steel Construction. One East Wacker Drive. IL.

[2] ACI Committee 318. (2011). *Building Code Requirements for Structural Concrete (ACI 318-11M) and Commentary*. American Concrete Institute. Farmington Hills, MI.

[3] Eom, T.S., Hwang, H.J., Park, H.G., Lee, C.N. and Kim, H.S., (2013). *Flexural test for steel-concrete composite members using prefabricated steel angles*. Journal of Structural Engineering, Vol. 140(4), p.04013094.

[4] Kim, C.G., Park, H.G., Hong, G.H. and Kang, S.M., (2016). *Shear Strength of Composite Beams with Dual Concrete Strengths*. ACI Structural Journal, 113(2), p.263.

[5] Kim, C.G., Park, H.G., Hong, G.H., Kang, S.M. and Lee, H., (2017). *Shear Strength of Concrete Composite Beams with Shear Reinforcements*. ACI Structural Journal, 114(4), p.827.

[6] Loov, R.E. and Patnaik, A.K. (1994). *Horizontal Shear Strength of Composite Concrete Beams*. PCI JOURNAL, Vol. 39(1), pp.48-69.

[7] Mattock, A.H. and Hawkins, N.M. (1972). *Shear transfer in reinforced concrete—Recent research*. PCI Journal, 17(2), pp.55-75.

[8] Weng, C.C., Yen, S.I. and Chen, C.C., (2001). *Shear strength of concrete-encased composite structural members*. Journal of structural engineering, 127(10), pp.1190-1197.

[9] Juang, J.L. and Hsu, H.L., (2006). *Bond mechanism effect on the flexural behavior of steel reinforced concrete composite members*. Steel and Composite Structures, 6(5), pp.387-400.

References

Appendix A : Exact Method of Plastic Moment Calculation in Angle Truss Composite Beam

Case 1 : $c > l_1$

The location of neutral axis is below top angles. So, all area of top angle is in compression.

Table A-1 Material strengths and area of each elements in Case 1

	Material Strength (MPa)	Area of Elements (mm^2)	Force
Concrete	$0.85 f_{ck}$	$ab = \beta_1 cb$	C_c
Top angle	F_{ya}	A_a	C_a
Top rebar	F_{yrc}	A_{src}	C_r
Bottom angle	F_{ya}	A_a	T_a
Bottom rebar	F_{yrt}	A_{srt}	T_r

From plastic stress, each force can be calculated by the product of area and yield stress ($0.85 f_{ck}$ in concrete).

$$C_c = 0.85 f_{ck} ab \tag{A-1}$$

$$C_a = A_a F_{ya} \tag{A-2}$$

$$C_r = A_{src} F_{yrc} \tag{A-3}$$

$$T_a = -A_a F_{ya} \tag{A-4}$$

$$T_r = -A_{srt} F_{yrt} \tag{A-5}$$

From the force equilibrium,

$$C_c + C_a + C_r + T_a + T_r = 0 \tag{A-6}$$

$$c = -\frac{C_a + C_r + T_a + T_r}{0.85 f_{ck} \beta_1 b} \tag{A-7}$$

From **Eq.(A-7)**, neutral axis depth (c) can be calculated. Check if c is in the case 1 assumption, if not, go to case 2 and if so, the centroid of top angle can be calculated by **Eq.(A-8)** and **Figure A-1**. And plastic moment can be calculated by **Eq.(A-9)**.

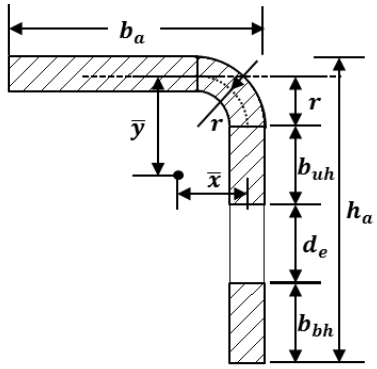

Figure A-1 The centroid of angle in case 1

$$\bar{y} = \left(\frac{t}{A_{a1}}\right)\left(b_{uh}\left(\frac{b_{uh}}{2} + r\right) + b_{bh}\left(\frac{b_{bh}}{2} + d_e + b_{uh} + r\right) + 0.363ur\right) \tag{A-8}$$

where, $u = \frac{\pi r}{2}$ one-forth center parameter of curved shape, $\bar{y}$ = the distance of angle's centroid, r = the center radiation of curved part, t = the thickness of angle, A_{a1} = the area of single angle, b_{uh} = the length of upper bolt hole, b_{bh} =

the length of below bolt hole, d_e = the diameter of bolt hole, b_a = the width of angle, and h_a = the height of angle.

$$M_p = C_c\left(\frac{h}{2}-\frac{a}{2}\right)+C_a\left(\frac{h}{2}-\overline{y_c}\right)+C_r\left(\frac{h}{2}-d_{cr}\right) + T_a\left(\frac{h}{2}-d_{ta}\right)+T_r\left(\frac{h}{2}-d_{tr}\right) \quad \text{(A-9)}$$

where, $a=\beta_1 c$, $\overline{y_c}$ = the depth of the centroid of top angles, d_{cr} = the depth of the center of top rebars, d_{ta} = the depth of the centroid of bottom angles, d_{tr} = the depth of the center of bottom rebars

Case 2 : $l_2 < c < l_1$

The location of neutral axis is in angle's web. So, the area of top angle is divided into two sections (compression, tension).

Table A-2 Strength and area of each elements in Case 2

	Material Strength (MPa)	Area of Elements (mm^2)	Force
Concrete	$0.85 f_{ck}$	$ab = \beta_1 cb$	C_c
Top angle (Comp.)	F_{ya}	$A_a - 2(l_1 - c)t$	C_{ta}
Top angle (Tens.)	F_{ya}	$2(l_1 - c)t$	T_{ta}
Top rebar	F_{yrc}	A_{src}	C_r
Bottom angle	F_{ya}	A_a	T_a
Bottom rebar	F_{yrt}	A_{srt}	T_r

The difference with previous one is only top angle's division. The compression zone of angle shows the force which magnitude is C_{ta}. The tension zone of angle acts the force which magnitude is T_{ta}.

$$C_{ta} = \left(A_a - 2(l_1 - c)t\right)F_{ya} \tag{A-10}$$

$$T_{ta} = -2(l_1 - c)tF_{ya} \tag{A-11}$$

The force equilibrium equation (**Eq.(A-12)**) can be written using **Eq.(A-1),(A-3),(A-4),(A-5),(A-10)**, and **(A-11).**

$$C_c + C_{ta} + C_r + T_{ta} + T_a + T_r = 0 \tag{A-12}$$

$$\left(0.85 f_{ck} \beta_1 b + 4tF_{ya}\right)c = -\left(C_r + T_r\right) + 4l_1 tF_{ya} \tag{A-13}$$

$$c = \frac{4l_1 tF_{ya} - C_r - T_r}{0.85 f_{ck} \beta_1 b + 4tF_{ya}} \tag{A-14}$$

From **Eq.(A-14)**, neutral axis depth (c) can be calculated. Check if c is in the Case 2 assumptions, if not, go to case 3 and,

If so, the centroid of top angle can be calculated by **Eq.(A-15), (A-16)**, and **Figure A-2**.

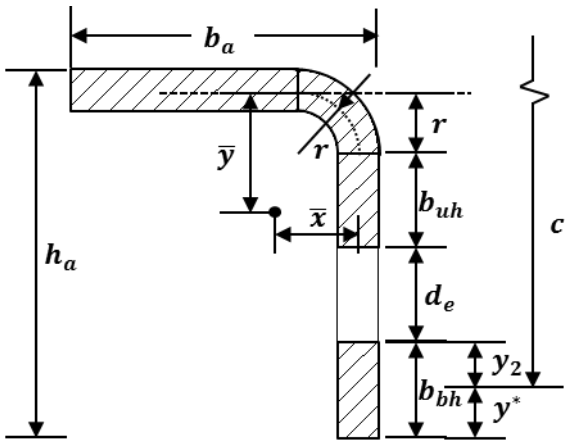

Figure A-2 The centroid of angle in case 2

$$\overline{y_c} = \left(\frac{t}{A_{a1} - yt} \right) \left(\begin{array}{l} b_{uh} \left(\frac{b_{uh}}{2} + r \right) + y_2 \left(\frac{y_2}{2} + d_e + b_{uh} + r \right) \\ +0.363ur \end{array} \right) \qquad \text{(A-15)}$$

where, $u = \frac{\pi r}{2}$, $y_2 = c - l_1 - \frac{t}{2} - r - b_{uh} - d_e$, $\overline{y_c}$ = the centroid of angle's compression zone.

$$\overline{y_t} = c + \frac{y^*}{2} \qquad \text{(A-16)}$$

where, $y^* = b_{bh} - y_2$, $\overline{y_t}$ = the centroid of angle's tension zone.

And plastic moment can be calculated by **Eq.(A-17)**

$$\begin{aligned} M_p = {} & C_c \left(\frac{h}{2} - \frac{a}{2} \right) + C_{ta} \left(\frac{h}{2} - d_{cta} \right) + C_r \left(\frac{h}{2} - d_{cr} \right) \\ & + T_{ta} \left(\frac{h}{2} - d_{tta} \right) + T_a \left(\frac{h}{2} - d_{ta} \right) + T_r \left(\frac{h}{2} - d_{tr} \right) \end{aligned} \qquad \text{(A-17)}$$

Case 3 : $l_3 < c < l_2$

The location of neutral axis is in angle's web. So, the area of top angle is divided into two sections (compression, tension).

Table A-3 Strength and area of each elements in Case 3

	Material Strength (MPa)	Area of Elements (mm^2)	Force
Concrete	$0.85 f_{ck}$	$ab = \beta_1 cb$	C_c
Top angle (Comp.)	F_{ya}	$A_a - 2b_{bh}t$	C_{ta}
Top angle (Tens.)	F_{ya}	$2b_{bh}t$	T_{ta}
Top rebar	F_{yrc}	A_{src}	C_r
Bottom angle	F_{ya}	A_a	T_a
Bottom rebar	F_{yrt}	A_{srt}	T_r

The basic procedure is the same with the previous one. The only difference is the magnitude of C_{ta} and T_{ta} .

$$C_{ta} = \left(A_a - 2b_{bh}t\right) F_{ya} \tag{A-18}$$

$$T_{ta} = -2b_{bh}tF_{ya} \tag{A-19}$$

From force equilibrium using Eq.(A-12)

$$C_c + C_{ta} + C_r + T_{ta} + T_a + T_r = 0 \tag{A-12}$$

$$(0.85 f_{ck} \beta_1 b) c = -(C_{ca} + C_r + T_{ta} + T_a + T_r) \tag{A-20}$$

$$c = -\frac{C_{ta} + C_r + T_{ta} + T_a + T_r}{0.85 f_{ck} \beta_1 b} \tag{A-21}$$

From **Eq.(A-21)**, neutral axis depth (c) can be calculated. Check if c is in the Case 3 assumptions, if not, go to case 4 and,

If so, the centroid of top angle can be calculated by Eq.**(A-22),(A-23)**, and **Figure A-3.**

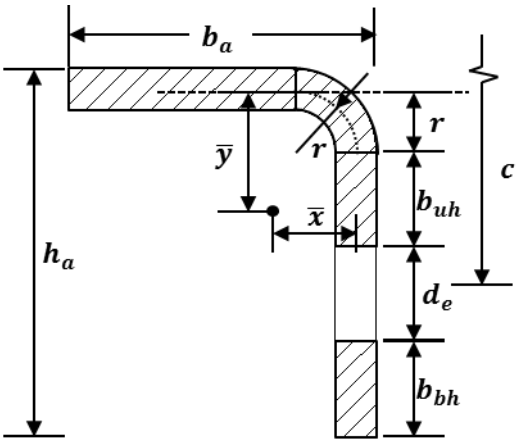

Figure A-3 The centroid of angle in case 3

$$\overline{y_c} = \left(\frac{t}{A_{a1} - b_{bh} t} \right) \left(b_{uh} \left(\frac{b_{uh}}{2} + r \right) + 0.363 ur \right) \tag{A-22}$$

$$\overline{y_t} = l_2 + \frac{b_{bh}}{2} \tag{A-23}$$

Case 4 : $l_4 < c < l_3$

The location of neutral axis is in angle's web. So, the area of top angle is divided into two sections (compression, tension).

Table A-4 Strength and area of each elements in Case 4

	Material Strength (MPa)	Area of Elements (mm^2)	Force
Concrete	$0.85 f_{ck}$	$ab = \beta_1 cb$	C_c
Top angle (Comp.)	F_{ya}	$A_a - 2b_{bh}t - 2(l_3 - c)t$	C_{ta}
Top angle (Tens.)	F_{ya}	$2b_{bh}t + 2(l_3 - c)t$	T_{ta}
Top rebar	F_{yrc}	A_{src}	C_r
Bottom angle	F_{ya}	A_a	T_a
Bottom rebar	F_{yrt}	A_{srt}	T_r

The basic procedure is the same with the previous one. The only difference is the magnitude of C_{ta} and T_{ta}.

$$C_{ta} = \left(A_a - 2b_{bh}t - 2(l_3 - c)t\right)F_{ya} \tag{A-24}$$

$$T_{ta} = -\left(2b_{bh}t + 2(l_3 - c)t\right)F_{ya} \tag{A-25}$$

From force equilibrium using **Eq.(A-12)**

$$C_c + C_{ta} + C_r + T_{ta} + T_a + T_r = 0 \tag{A-12}$$

$$\left(0.85 f_{ck} \beta_1 b + 4tF_{ya}\right)c = 4b_{bh}tF_{ya} + 4l_3 tF_{ya} - \left(C_r + T_r\right) \tag{A-26}$$

$$c = \frac{4b_{bh}tF_{ya} + 4l_3 tF_{ya} - C_r - T_r}{0.85 f_{ck} \beta_1 b + 4tF_{ya}} \tag{A-27}$$

From **Eq.(A-27)**, neutral axis depth (c) can be calculated. Check if c is in the Case 4 assumptions, if not, go to case 5 and, if so, the centroid of top angle can be calculated by **Eq.(A-28), (A-29)**, and **Figure A-4.**

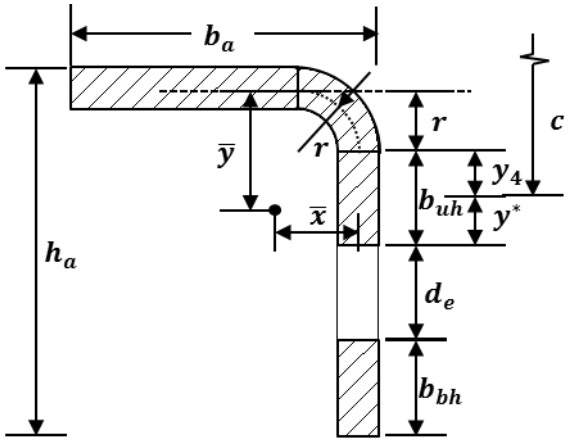

Figure A-4 The centroid of angle in case 4

$$\overline{y_c} = \left(\frac{t}{A_{a1} - b_{bh}t - yt}\right)\left(b_{uh}\left(\frac{b_{uh}}{2} + r\right) + y_4\left(\frac{y_4}{2} + r\right) + 0.363ur\right) \tag{A-28}$$

where, $u = \frac{\pi r}{2}$, $y_4 = c - l_1 - \frac{t}{2} - r$, and $y^* = b_{uh} - y_4$

$$\overline{y_t} = c + \frac{y^* + b_{bh}}{2} + d_e \tag{A-29}$$

Case 5 : $l_a < c < l_4$

The location of neutral axis is in angle's flange. So, the area of top angle is divided into two sections (compression, tension).

Table A-5 Strength and area of each elements in Case 5

	Material Strength (MPa)	Area of Elements (mm^2)	Force
Concrete	$0.85 f_{ck}$	$ab = \beta_1 cb$	C_c
Top angle (Comp.)	F_{ya}	$b_a (c - l_a)$	C_{ta}
Top angle (Tens.)	F_{ya}	$A_a - b_a (c - l_a)$	T_{ta}
Top rebar	F_{yrc}	A_{src}	C_r
Bottom angle	F_{ya}	A_a	T_a
Bottom rebar	F_{yrt}	A_{srt}	T_r

The basic procedure is the same with the previous one. The only difference is the magnitude of C_{ta} and T_{ta}.

$$C_{ta} = b_a (c - l_a) F_{ya} \tag{A-30}$$

$$T_{ta} = -\left(A_a - b_a (c - l_a)\right) F_{ya} \tag{A-31}$$

From force equilibrium using Eq.(A-12).

$$C_c + C_{ta} + C_r + T_{ta} + T_a + T_r = 0 \tag{A-12}$$

$$\left(0.85 f_{ck} \beta_1 b + 2 b_a F_{ya}\right) c = 2 b_a l_a F_{ya} - \left(C_r + 2T_a + T_r\right) \tag{A-32}$$

$$c = \frac{2 b_a l_a F_{ya} - C_r - 2T_a - T_r}{0.85 f_{ck} \beta_1 b + 2 b_a F_{ya}} \tag{A-33}$$

From **Eq.(A-33)**, neutral axis depth (c) can be calculated. the centroid of top angle can be calculated by **Eq.(A-34), (A-35)** and, **Figure A-5.**

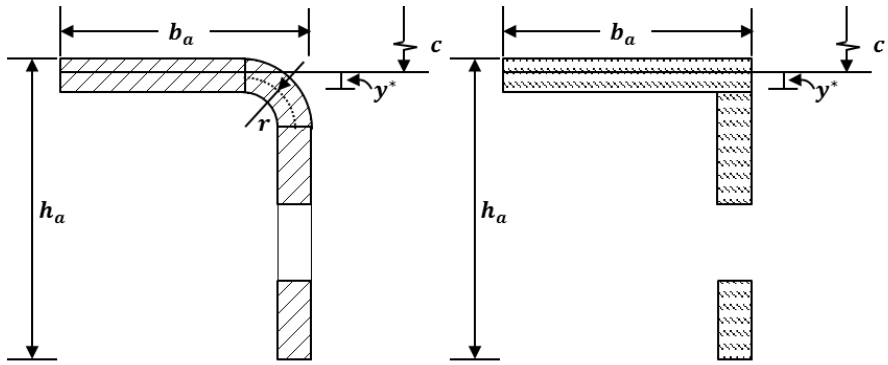

Figure A-5 The centroid of angle in case 5 using equivalent angle section

$$\overline{y_c} = l_a + \frac{c - l_a}{2} \tag{A-34}$$

$$\overline{y_t} = \left(\frac{A_1}{A_{a1}}\right)\left(c + \frac{y^*}{2}\right) + \left(\frac{A_2}{A_{a1}}\right)\left(c + y^* + \frac{h_a - t}{2}\right) \tag{A-35}$$

where, $A_t = b_a\left(c - l_a\right)$, $A_1 = b_a y^*$, $A_2 = A_{a1} - A_t - A_1$,

$y_4 = c - l_1 - \frac{t}{2} - r$, and $y^* = b_{uh} - y_4$

Appendix B : Simple Method of Plastic Moment Calculation in Angle Truss Composite Beam

Case 1 : $c > l_1$

The location of neutral axis is below top angles. So, all area of top angle is in compression. This is the same with Case 1 in exact method without $\bar{y}$ calculation. From, force equilibrim equation can be rewrited as Eq.(B-1), (B-2). The neutral axis depth are got in Eq.(B-3)

$$C_c + C_a + C_r + T_a + T_r = 0 \tag{B-1}$$

$$(0.85 f_{ck} \beta_1 b)c = -(C_a + C_r + T_a + T_r) \tag{B-2}$$

$$c = -\frac{C_a + C_r + T_a + T_r}{0.85 f_{ck} \beta_1 b} \tag{B-3}$$

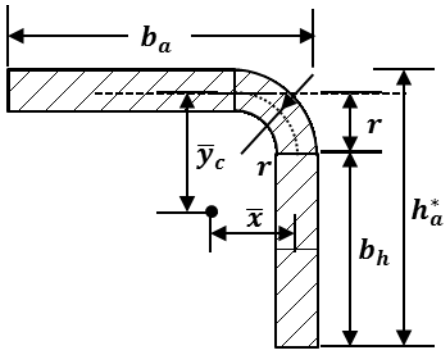

Figure B-1 The centroid of angle in case 1 (simple)

$$\bar{y}_c = \left(\frac{t}{A_{a1}}\right)\left((b_{uh} + b_{bh})\left(\frac{b_{uh} + b_{bh}}{2} + r\right) + 0.363ur\right) \tag{B-4}$$

where, $u = \frac{\pi r}{2}$

$b_h = b_{uh} + b_{bh}$

Case 2 : $l_2 < c < l_1$

The location of neutral axis is in angle's web. So, the area of top angle is divided into two sections (compression, tension). This is the same with Case 2 in exact method without $\bar{y}_c, \bar{y}_t$ calculation.

From, force equilibrim equation can be rewrited as Eq.(B-5), (B-6). The neutral axis depth is got in Eq.(B-7).

$$C_c + C_{ta} + C_r + T_{ta} + T_a + T_r = 0 \tag{B-5}$$

$$\left(0.85 f_{ck} \beta_1 b + 4 t F_{ya}\right) c = -(C_r + T_r) + 4 l_1 t F_{ya} \tag{B-6}$$

$$c = \frac{4 l_1 t F_{ya} - C_r - T_r}{0.85 f_{ck} \beta_1 b + 4 t F_{ya}} \tag{B-7}$$

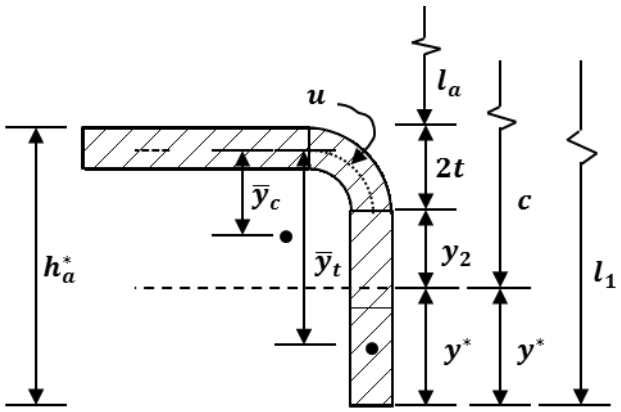

Figure B-2 The centroid of angle in case 2 (simple)

$$\bar{y}_c = \left(\frac{t}{A_{a1} - y^* t}\right)\left(y_2\left(\frac{y_2}{2} + r\right) + 0.363 u r\right) \tag{B-8}$$

where, $y_2 = c - l_a - 2t$

$y^* = l_1 - c$

$$\bar{y}_t = c + \frac{y^*}{2} \tag{B-9}$$

Case 5 : $l_a < c < l_2$

The location of neutral axis is in angle's flange. So, the area of top angle is divided into two sections (compression, tension). This is the same with Case 5 in exact method without $\bar{y}$ calculation.

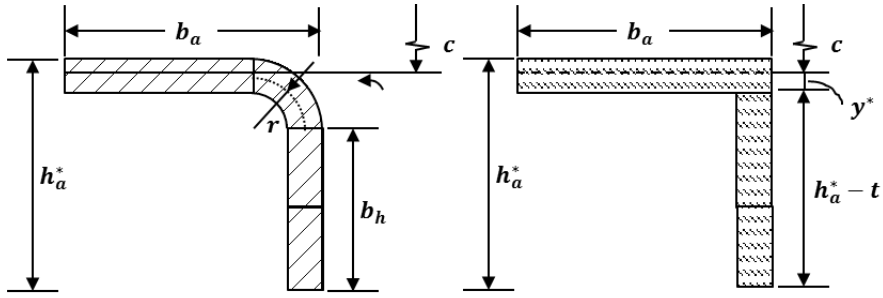

Figure B-3 The centroid of angle in case 5 using equivalent angle section

$$\bar{y}_c = l_a + \frac{c - l_a}{2} \tag{B-10}$$

$$\bar{y}_t = \left(\frac{A_1}{A_t}\right)\left(c + \frac{y^*}{2}\right) + \left(\frac{A_2}{A_t}\right)\left(c + y^* + \frac{h_a^* - t}{2}\right) \tag{B-11}$$

where $y^* = l_2 - c$

$A_1 = b_a y^*$

$A_2 = A_{a1} - A_c - A_1$

$A_c = b_a(c - l_a)$

국문 초록

건설현장에서 기술의 고도화, 인건비 증가 등으로 현장에서의 노무를 줄이고 공장에서 제작해오는 프리캐스트공법이 많은 환영을 받고 있다. 또한 구조부재로써는 전통적으로 사용하던 일반 철근과 콘크리트만 사용하는 것이 아닌, 강재의 사용으로 효율성을 높이려는 여러 시도들이 이루어 지고있다. 이 연구에서 제시하는 앵글형 합성보는 일종의 매입형 합성보로써, 강판을 절곡한 절곡앵글을 사용하여 트러스를 구성하고 하부에 U형 프리캐스트를 타설하여 공장제작을 한다. 하부 프리캐스트 콘크리트는 거푸집을 대용해 현장 노무를 줄이게 된다. 이후 현장으로 운반되어 기둥에 거치되며, 이후 현장타설 콘크리트와 일체화 된다. 이러한 시스템은 내부 앵글트러스의 존재로 인해 시공시 단면의 유효 깊이가 깊어지므로, 프리캐스트 콘크리트 물량을 획기적으로 줄일수 있으므로 경제적이다. 또한 시공시에도 가벼운 양중무게로 편의성을 더해줄 수 있는 장점이 있다.

개발된 앵글형 합성보의 휨 및 전단 실험을 통하여 구조성능을

검증하고자 하였고, 기존에 사용되는 설계기준의 예상강도 값과 비교분석하였다. 앵글형 합성보의 휨실험에서는 부착강도를 평가한 기존식으로 설계하였을 때 잘 맞는 것을 알 수 있었고, 설계 휨강도 역시도 획득하였다. 다만, 제안한 시공 단면에서 볼트의 미끄러짐의 발생으로 처짐이 과다하게 발생하였다. 이부분에 대해서는 추가적인 연구가 필요하다. 전단실험에서는 매입되는 앵글트러스의 웨브재를 일반 철근콘크리트의 전단철근화하여 계산하였고, 실험 결과는 예상강도에 비해 다소 못미치거나 잘 맞는 것으로 나타났다. 예상강도에 비해 낮게 나온 실험체의 파괴 모드가 대각인장파괴와 달랐다. 이는 앵글 트러스의 상현재와 상부 콘크리트 계면에서의 전단부착파괴에 의한 것으로 분석되었다. 부착 파괴가 발생하지 않는 경우에는 내부 복부부재가 모두 항복하는 것으로 확인되어 전단강도 산정시에 고려가 가능할 수 있다. 다만 트러스의 복부재는 볼트에 의해 연결되기 때문에, 그 전단강도의 상한값을 볼트 전단강도로 하였다.

이러한 구조성능평가를 통하여 앵글형 합성보라는 일종의 매입형

합성보의 대한 휨성능 및 구조성능을 확인할 수 있었고, 매입형 합성보의 전단강도 계산시에 내부 강재의 기여분을 더할 수 있다는 결론을 얻었다.

주요어 : 매입형 합성부재, 전단 강도, 휨 강도, 프레스트레스트 보, 프리캐스트, 앵글 트러스

학번 : 2016- 21088